MODELING THE IMPACTS OF GREEN INFRASTRUCTURE ON *E. COLI* IN THE VILLAGE CREEK WATERSHED, TEXAS

by

HOLLY ANNE GOULD

Bachelor of Science, 2018
University of South Carolina
Columbia, South Carolina

Submitted to the Graduate Faculty of the
College of Science and Engineering
Texas Christian University
in partial fulfillment of the requirements
for the degree of

Master of Science

July 2021

ACKNOWLEDGEMENTS

First, I would like to give a special thank you to my thesis advisor, Dr. Gehendra Kharel, for allowing me to work on this thesis project. Thank you for teaching me along the way and providing me with much-needed guidance. I truly appreciate all of the support, patience, and encouragement you provided me over the past two years! I am incredibly appreciative and thankful to my committee members, Becky Johnson, P.G., and Dr. Jaehak Jeong, for their tremendous contribution and advisement to my thesis project and writing.

I would also like to express my appreciation and gratitude to Heather Firn from Trinity River Authority, and Aaron Hoff, from Tarrant Regional Water District, for providing information and data on the Village Creek-Lake Arlington watershed. Their knowledge of Village Creek was constructive throughout this research project.

Additionally, I would like to thank the faculty, staff, and graduate students of the environmental sciences department at Texas Christian University. Everyone has provided me with tremendous support and assistance throughout this process. Finally, I would like to thank my family and friends for all of their encouragement and support over the past two years.

TABLE OF CONTENTS

LIST OF FIGURES

LIST OF TABLES

MODELING THE IMPACTS OF GREEN INFRASTRUCTURE ON *E. COLI* IN THE VILLAGE CREEK WATERSHED, TEXAS

College of Science and Engineering

Thursday, July 29, 2021

Section I: Introduction

Water is one of the most valuable natural resources on Earth and is essential for all species and ecosystems. Of all water on earth, about 97.5% is saltwater, and the remaining 2.5% is freshwater (Brears, 2017). Surface water is water found in rivers, lakes, and streams and makes up 0.3% of available freshwater. Groundwater is the water stored underground in soils, rocks, and aquifers, making up 29.7% of freshwater. Freshwater resources are primarily extracted from surface water and groundwater to be used for drinking, energy, irrigation, domestic or industrial activity (Dieter et al., 2018). In the U.S., freshwater makes up about 87% of the total water extracted for societal use, and 70% of this water is sourced from surface waters (Dieter et al., 2018). The hydrologic cycle transports water through the earth's surface and atmosphere, supplying water resources for the population and ecosystems. Precipitation replenishes surface water and groundwater, where stormwater infiltrates into the soil or migrates to nearby waterbodies. Anthropogenic land use and human activity directly influence the hydrology of an area, which further affects the quantity and quality of water available. Freshwater has limited availability; therefore, it is crucial to protect the water resources currently available.

One of the examples of human activity that interferes with our water resources by altering natural hydrology and introducing new physical, chemical, and biological properties into the environment is urbanization (Hibbs and Sharp, 2012). Through urbanization, an area becomes more developed for industrial, commercial, transportation, and residential uses. This development replaces the natural landscape with impervious surfaces, solid materials used for highways, sidewalks, parking lots, and buildings. These developments alter natural hydrological processes and lead to water quantity problems (e.g., urban flooding). Additionally, urban areas accumulate higher concentrations of pollutants due to increased human activities leading to water pollution (e.g., elevated bacteria concentrations) in urban and peri-urban water resources. In the U.S., 13% of measured rivers, 18% of lakes, and 32% of estuaries have been classified as 'impaired' in water quality standards due to stormflow carrying and discharging pollutants (Jaber, 2015).

The global population will increase from 7.8 billion in 2020 to 9.7 billion in 2050, growing global water demand by 55% (United Nations, 2019). In addition, by 2050, projections show that about 68% of the population will reside in urban areas, which is a 13% increase from 2018 urban residence (United Nations, 2019). This urban population growth will increase the demand for urban space, with projections showing more than a tripling of urban land cover by 2050 (United Nations, 2019). These characteristics of urbanization can impose negative consequences on the water in urban and peri-urban watersheds (Roser, 2020). Therefore, for the sustainable management of water resources and improving water quality, there is a need for problem-solving strategies that address urban water challenges.

Section II: Background

A drainage basin or watershed is an area where precipitation that falls evaporates, infiltrates, or flows overland, ultimately reaching streams and discharging to water bodies. Water exists in all phases within a drainage basin through the hydrologic cycle (Fig. 1), which can also occur at a watershed scale. During a precipitation event over a natural landscape, rainfall is intercepted by vegetation, evaporates to the atmosphere, enters water bodies, or falls on the land surface. On the land surface, stormwater can take various pathways: infiltrates to become soil moisture, infiltrates to be absorbed by plants, infiltrates deeper into the subsurface, resupplying groundwater and aquifers, or runs over the land as surface runoff to accumulate in surface water bodies (Brears, 2017). The infiltrating stormwater may also flow laterally in the subsurface, typically discharging to nearby streams and rivers as baseflow. Surface runoff, also known as stormflow or overland flow, is the excess stormwater that flows along the land surface into nearby water bodies. The joint baseflow and stormflow make up the total streamflow, which is the total volume of water discharged into the surface water body. After a storm event, the maximum streamflow in an area during the storm duration is known as the peak flow. Streamflow carries varying amounts of nutrients, sediments, bacteria, and other materials along with it (Brears, 2017).

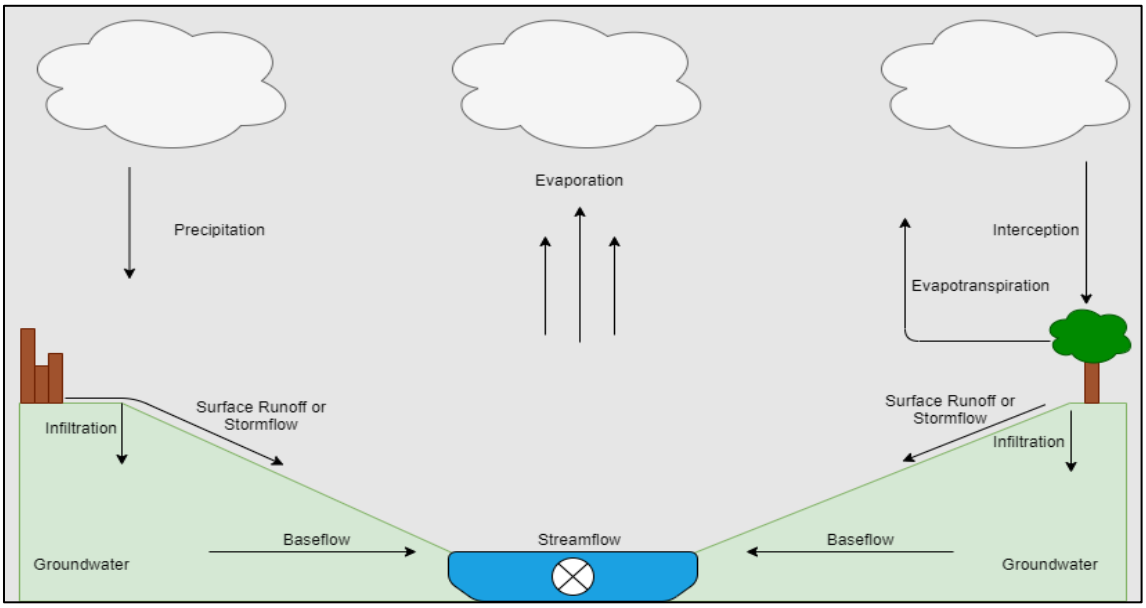

Figure 1. Hydrologic cycle in a watershed

Natural and anthropogenic conditions have an influence on the processes and quality of the hydrologic cycle. Natural conditions include temperature, land cover, vegetation, and the physical and chemical composition of soils. For example, higher temperature increases the rate of evaporation, eventually leading to more precipitation (Brears, 2017). Additionally, anthropogenic activities intrude on the earth's natural systems by altering surface temperature, land, and vegetation cover and by introducing or altering biological, physical, and chemical properties to the system (Hibbs and Sharp, 2012). Studies have shown that human-induced climate change, land degradation, industrialization, intensive agriculture, and urbanization have disproportionately changed global hydrological regimes (Akhter and Hewa, 2016; Hagemann et al., 2013; Hibbs and Sharp, 2012; Renner et al., 2014)

Urban areas can often be characterized by high population densities, impervious land cover and infrastructure, and various human activities; however, these are characteristics that alter the hydrology and water quality for an area (Liu et al., 2016). Urban areas have infrastructure developments for industrial, commercial, transportation, and residential purposes that alter the physical landscape by replacing native vegetation and land cover with impervious surfaces (e.g., concrete surfaces, buildings) (Hibbs and Sharp, 2012; Nguyen et al., 2019). Impervious surfaces limit stormwater's access to vegetated areas, where infiltration would naturally occur. Consequently, the stormwater accumulates on the impervious surfaces, resulting in high water volumes on the surface and increased stormflow (Caldwell et al., 2012; Liu et al., 2016). Additionally, the lack

of vegetation decreases rainfall interception by plants, resulting in larger volumes of stormwater reaching the land surface at a faster rate (Houng Li et al., 2009). Generally, 40% of stormwater evaporates in natural landscapes, about 50% infiltrates, and 10% remains as stormflow, which is discharged to nearby surface waters, contributing to total streamflow (Arnold and Gibbons, 1996; Brears, 2017). However, impervious cover interferes with these processes and alters the distribution of stormwater (Liu et al., 2016). In areas with 75-100% impervious cover, about 30% of precipitation evaporates, while only 15% of the stormwater can infiltrate the ground and 55% becomes stormflow (Arnold and Gibbons, 1996; Brears, 2017). The lower infiltration rate and higher stormflow in urban areas lead to excess stormflow and reduced groundwater recharge (Hibbs and Sharp, 2012; Liu et al., 2016). Studies have shown that higher impervious surface coverage can increase flooding volumes up to 162%, large-scale floods by 100%, and the occurrence of small-scale floods by 200% (Konrad, 2016; Shiqiang Du, 2015). One study in the San Antonio and Guadalupe River Basin found increased impervious cover from urbanization increased flood peaks from 3% to 30% (Shao et al., 2020). Hu and Shrestha (2020) did a modeling study for a watershed in St. Louis, Missouri, where they found that the 11.21% increase in impervious cover resulted in a 126 - 176% increase in peak discharge from storm events (Hu and Shrestha, 2020). Additionally, Shiqiang Du, et. al (2015) found that 63% increase in impervious surface coverage in a watershed in Shenzhen, China increased peak discharge and flood volume by 140-162% (Shiqiang Du, 2015). In addition to the increased frequency and intensity of flood events, the excess accumulation of stormwater in urban areas may degrade surrounding habitat, land, and community through high erosion and infrastructure damage (EPA, 2019).

Urbanization also introduces high concentrations of both point and nonpoint source pollutants that can be transported to surface water through stormflow and result in water quality impairments (Hibbs and Sharp, 2012; Osman et al., 2019). Point source pollutants can be traced to a specific location, such as industrial wastes, landfills, storage tanks, and factories where they can be monitored (Brears, 2017). Nonpoint source pollutants, the most common urban polluter, are released from various sources, making it difficult to track to a specific location and challenging to monitor and control (Brears, 2017). Common urban pollutants that result from lawn fertilizers, pet and yard wastes, sewage systems, wastewater, and construction and transportation activities include bacteria and pathogens, nitrogen (N), phosphorous (P), bacteria, oil, grease, sediments, and heavy metals (Hibbs and Sharp, 2012; Hobbie et al., 2017; Jaber, 2015; Lian et al., 2019; Liu et al., 2016). These pollutants adhere to and build up on impervious surfaces (Rezaei et al., 2019). After a storm event, stormflow

washes off these built-up pollutants, discharging them into neighboring water bodies (Brears, 2017). Thus, high stormflow volumes in urban areas where pollutants often accumulate at higher concentrations can transport and increase pollutant concentrations in surface water. Therefore, stormflow is one of the leading causes of water quality impairments in many developed regions, including the U.S., Australia, and European nations (Arnold and Gibbons, 1996; EPA, 2019; Levin et al., 2002; Pistocchi, 2020; Sidhu et al., 2013).

According to the U.S. EPA, about 55% of all the assessed rivers and streams in the U.S. are classified as impaired (U.S. EPA, 2017) caused primarily by pathogens, sediment, and nutrients such as N and P. Pathogens are bacteria including fecal coliform, which can be sourced from human effluent, pet, wildlife, or livestock waste. Exposure to pathogenic bacteria can cause disease or illness and threaten public health (Hathaway et al., 2009; U.S. EPA, 2017). Pathogenic pollution is the leading cause of water quality impairments, polluting about 17% of the miles from assessed rivers and streams (EPA, 2017a). Of the types of pathogen fecal coliforms, *Escherichia coli (E. coli*) is the primary pollutant, causing impairments to 10% of the assessed rivers and streams in the U.S. (EPA, 2017a). When a water body tests positive for *E. coli*, this may indicate that the water body has fecal contamination, generally sourced from sewage effluent or animal waste.

In urban and semi-urban watersheds, sewage and waste can be a major influence on water quality. One way in which sewage can reach water bodies is through sanitary sewer overflows (SSOs) caused by high stormflow volumes and flood waters. SSOs occur when stormwater fills sewage systems, causing a mixture of storm and sewage water to overflow onto impervious surfaces and subsequently be transported to the neighboring water bodies (Levin et al., 2002; Liu et al., 2015; Rezaei et al., 2019). Another route is through the failing of septic systems, which are types of on-site sewage facilities, found in about 25% of U.S. homes, with some southern states (North Carolina, South Carolina, Georgia, Alabama) having an average between 37-48% (Ahmed et al., 2005; Sowah et al., 2017; Withers et al., 2014). Generally placed underground, these systems are designed to treat effluent where the liquids are released and infiltrated into the soil and can be absorbed by plants or recharge groundwater. When septic systems are properly placed, constructed, and maintained, they successfully remove about 70% to 90% of pollutants (Withers et al., 2014). However, septic systems can release contaminants that are not removed by the system when improperly installed and poorly maintained. When there is a failing septic system, the untreated wastewater can release nutrients and bacteria (*E. coli*) into groundwater or surface water from stormflow transport (Hoff et al., 2018; Sowah et al., 2017). Septic system failures usually result from various factors including, system age, improper and dense placement, extensive hydraulic or organic

loadings, soil conditions, infrastructure damage, or poor maintenance (EPA, 2005; Hoff et al., 2018; Sowah et al., 2017; Withers et al., 2014). Additionally, failures can go unnoticed for some time due to the lack of regulation (Withers et al., 2014). According to the U.S. EPA, the septic system failure rate is up to 25%, with some states reaching even higher rates (EPA, 2005). Failure rate estimations for states have been as high as 50-70% in Minnesota and as low as 0.4% in Wyoming (U.S. EPA, 2002). Generally, counties in the U.S. report about 11% or 12% failure rate (Hoff et al., 2018; Withers et al., 2014).

Governments have developed strategies and enforced regulations in many countries about urban stormwater to address water problems (Bell et al., 2020; Saraswat et al., 2016). Regulatory programs like stormwater management, impervious surface limits, National Combined Sewer Overflow Control Strategy and the Clean Water Act (CWA) attempt to minimize pollution, stormwater issues, and the depletion of water in the U.S. These policies and programs address water issues and decrease the effects that human activity, like urbanization, has on the environment. The enforcement of these regulatory programs generated technologies, infrastructure, and management strategies, including green infrastructure (GI) practices to enhance water and environmental protection, allowing nations to grow, urbanize and evolve more sustainably.

GI practices are mitigation strategies that can be used in stormwater management projects and urban design to manage the implications of wet weather events (EPA, 2019). GI practices are also known as best management practices (BMPs) or low-impact developments (LIDs). The primary goal of GI practices is to control stormwater and pollution directly at the source by collecting stormwater and enhancing hydrologic processes, such as infiltration, evaporation, and groundwater recharge (EPA, 2019; Wen Liu, 2014). A variety of GI practices have been studied and implemented to reduce surface stormflow, discharge, and pollutant concentrations (Table 1) (EPA, 2017b).

Table 1. Green Infrastructure (GI) types and definitions as reported by NCCOG and the EPA (EPA, 2019; NCTCOG, 2021).

GI Category	GI Definitions	Image Description
Rainwater Harvesting	Rainfall collection and storage system, allowing for water collection and re-use.	 (NCTCOG, 2021)
Detention/retention Basins	Area that stores storm runoff and promotes infiltration and aquifer recharge	 (NCTCOG, 2021)
Rain Gardens or Bioretention Cells	Shallow, vegetated basins installed in unpaved areas to collect and absorb runoff from impervious surfaces.	 (EPA, 2019)
Permeable Pavements	Pavements constructed with porous openings that allow stormwater to pass through to reach a storage area or the natural surface.	 (EPA, 2019)

Green Roofs	Vegetated-covered roofs	 (EPA, 2019)
Bioswales or vegetated filter strips	Vegetated, mulched, or landscaped channels, which collect and transport stormwater.	 (EPA, 2019)
Sand Filters	Filters that infiltrate through a sand medium to remove trash and other pollutants.	 (NCTCOG, 2021)
Constructed Wetlands	Mimic of a natural wetland to capture and filter stormwater, while creating a habitat.	 (NCTCOG, 2021)

Studies have evaluated the use and benefits of GI practices in stormwater management projects. A study evaluating the inflows and outflows of surface stormflow from an installed bioretention cell, found localized reductions in stormflow and peak flows by 97% and cumulative pollutant removals (total sediment, N, and P) by 99% (Debusk and Wynn, 2011). When studying green roofs implemented in Portland, Oregon, Konrad (2009) found that they effectively reduced stormflow volumes by 56 - 64% (Kurtz, 2009). Furthermore, Hathaway et al. (2009) found that bioretention cells could reduce fecal coliform and *E. coli* concentrations by 89% and 92%, respectively (Hathaway et al., 2009). These studies demonstrate the effectiveness of individual GI practices within an area; however, combining multiple types of GI practices over a larger area can further reduce water quantity and contaminants. Zhang et al. (2019) estimated the potential effects of GI combinations by modeling a watershed and placing various GI practices throughout the study area. By modeling bioretention basins, infiltration trenches, porous pavements, and rainwater harvesting systems, the results found an average of 66% reductions in surface stormflow and 80% pollutant (N, P, sediment) reductions (Zhang et al., 2019).

When planning for GI practices, decision-makers need to understand an area's natural land cover and societal uses, such as topography, hydrology, soil, land use, surrounding infrastructure, population, etc. (Haifeng Jia et al., 2015). Additionally, it is vital to understand the GI practices and goals for water quantity and quality. Studies on maximizing the capabilities of GI practices highlight three factors to consider when planning: 1) spatial coverage, 2) the placement and distribution, and 3) the hydrologic properties of the GI practice (Fiori and Volpi, 2020; Fry and Maxwell, 2017). When a given area has more spatial coverage of GI practices there is more storage and infiltration; therefore, it can control high volumes of rainfall. By selecting optimal locations (placement and distributions), they can identify critical areas of concern where the GI practices can be effective (Di Matteo et al., 2017; Liu et al., 2017; Martin-Mikle et al., 2015). Identifying these locations includes assessing topography, groundwater depth, land use types, impervious cover, and locality to neighboring water bodies (Eaton, 2018; Saadat Foomani and Malekmohammadi, 2019). Fry, et al. (2017) compared rain gardens located along roads versus in residential lawns, where they found that road-side rain gardens reduced peak flows and stormflow by 8.58%, increased storage by 124.97%, and increased infiltration by 1.96% as compared to lawn gardens (Fry and Maxwell, 2017). Lastly, the hydrologic properties of the GI practices are crucial to meet the desired goals and can also play a role in their effectiveness during intense or mild storm events (Bai et al., 2018). The GI practices may not be as effective for all storm events; the intensity and duration of the rainfall may impact how much stormflow is collected (Bai et al., 2018; Fiori and Volpi,

2020; Zhang et al., 2019). To ensure that the GI will tackle the desired goals, tests and simulations can measure the efficiency of the GI practices.

Hydrological modeling is one way to perform these tests. Modeling tools are a representation of a natural system and can show hydrologic responses under various conditions. A model can be developed by inputting different data, demonstrating the physical and hydrologic conditions of a given area and the GI practices. A developed model can simulate climate scenarios and output estimates of the water quantity and quality under given scenarios or periods. Adding GI modules into the model under the same climatic conditions can estimate the effects of GI practices on water quantity and quality. A wide variety of hydrologic models can perform these tests. The Soil and Water Assessment Tool (SWAT) can estimate how changes to climate and land affect water resources in a watershed system. It has been used globally to model catchment systems, providing streamflow and non-point source pollution forecasting with various types of watersheds (Nguyen et al., 2018). The development of SWAT was originally for agricultural studies; however, studies are adapting the model to urban areas to quantify changes in water quantity and quality from GI practices. Nguyen, Recknagel, & Meyer (2018) used the SWAT to assess GI practices in an urban watershed and demonstrated that the combined implementation of buffer zones, constructed wetlands, and stabilized riverbanks could help control streamflow and the total P concentrations in the watershed (Nguyen et al., 2018).

As the population and urban development continue to grow, our water resources are at risk. Urban development, along with the demand for freshwater resources, will continue with the growing population. Therefore, it is crucial for society to develop sustainably by implementing new urban designs and management strategies, like GI practices, to reduce adverse effects on our water resources. Using hydrologic modeling tools for GI implementation and watershed protection, allowing stakeholders and researchers to make predictions and suggest solutions to urban water problems.

This thesis research aims to assess how implementing GI practices can affect E. *coli* in an urban watershed from a hydrological modeling perspective. The study area for this research is the Village Creek watershed, located in the North Central Plains (NCP) region of Texas (TX).

The NCP region of TX is experiencing changes to its water resources, urban growth trends, above-average rainfall events, and water quality impairments. From 2015 to 2040, the population in this region is projected to increase from 7 million to 10 million, encouraging the demand for development, with forecasts showing a potential doubling of impervious land cover by 2050 (NCTCOG, 2016; TRA, 2008; VNT, 2010).

Additionally, the NCP region has been experiencing more intense storm events, with rainfall volumes increasing by 15-20% per event (NCTCOG, 2016). In 2015, the region nearly doubled its annual average and received about 1,595 mm of rainfall, which caused flood damage to the area (NCTCOG, 2016). Furthermore, Texas, as a state, also has water quality impairment problems. About 42% of assessed rivers and streams are classified as impaired (EPA, 2017a). The primary cause of impairments is pathogenic bacteria, making up 27.5% of assessed rivers and streams (EPA, 2017a).

The Village Creek-Lake Arlington watershed is a 370 km^2 watershed situated in the NCP region (Hoff, 2019). Encompassing 28 river miles, the watershed stretches across Tarrant County and Johnson County, from Lake Arlington reservoir to Joshua, TX (Hoff, 2019). There are two primary urban areas encompassed in this watershed: Lake Arlington (north) and Burleson, TX (south). Lake Arlington is densely urbanized, located in the northern part of the watershed, and widely used for residential, recreation, and fishing purposes (Hoff, 2019). As a primary fresh water source for surrounding industries and communities, Lake Arlington supplies drinking water to approximately 500,000 people (Hoff, 2019). Lake Arlington's water supply originates from Village Creek, a northward-flowing tributary of the Trinity River (Fig. 2) (Hoff, 2019).

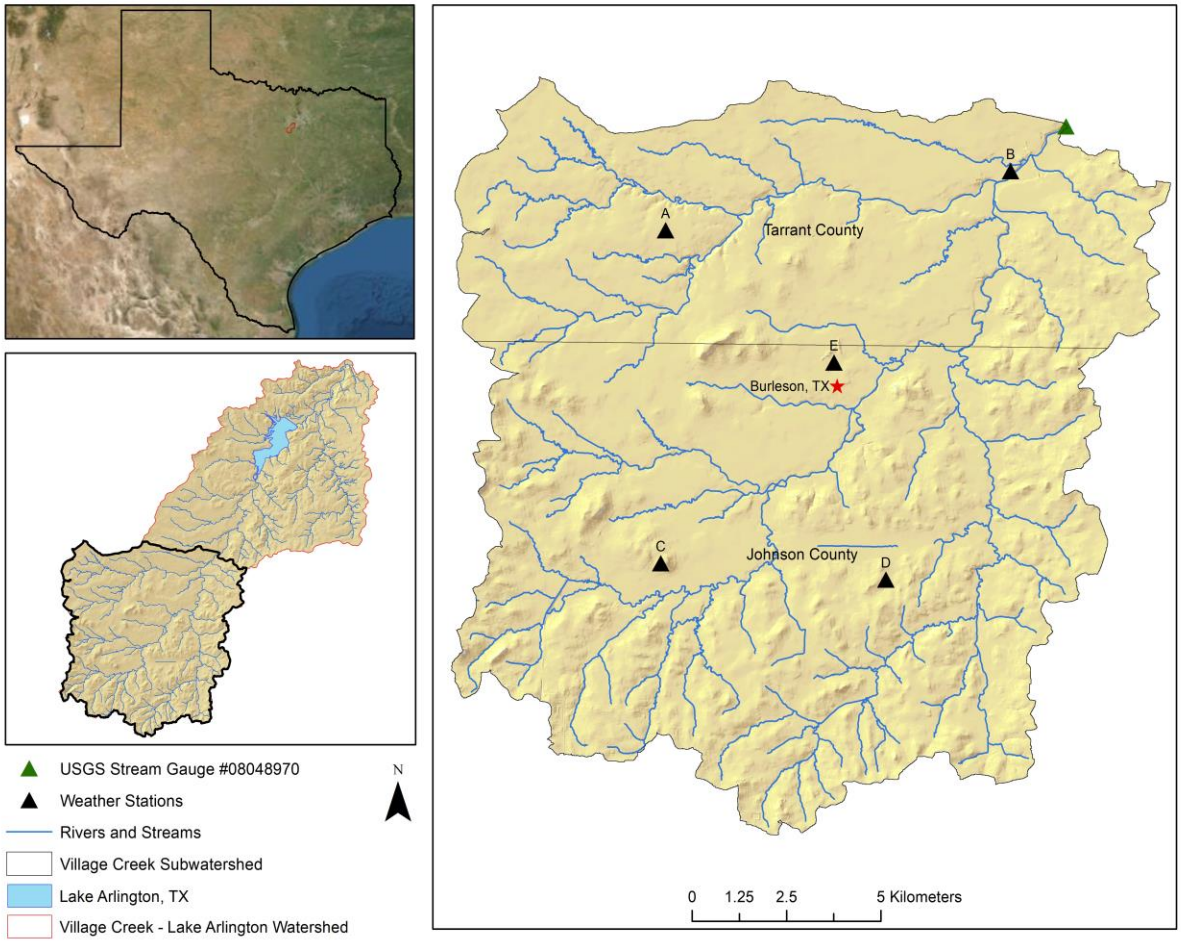

Figure 2. Study area, Village Creek watershed, located in north-central Texas region

Village Creek (VC) is a sub-watershed situated in the southern region of the overarching Village Creek-Lake Arlington watershed (Fig. 2). It is a semi-urban watershed with other mixed land-use types. Burleson, TX, is the primary urban center in the watershed, making up most of the urban land cover in Figure 3. Burleson, along with other cities in the NCP, is estimated to have a high potential for urban growth (Hoff, 2019). Based on the National Land Cover Database (NLCD) classification, all urban land cover types make up about ~30% of the watershed; this includes areas with a mixture of impervious and vegetated cover to areas that are 100% impervious cover (Fig. 3). Herbaceous land cover is another dominant land-use type, making up 30% of the watershed land use, including areas predominately covered with grass vegetation, which can be used for grazing and have minor maintenance. Additionally, the watershed consists of 27% forest and 12% agricultural land use for growing crops. The dominant soil type is hydrologic group D, which consists of more clay-like soils that contribute to lower infiltration rates and higher potential stormflow.

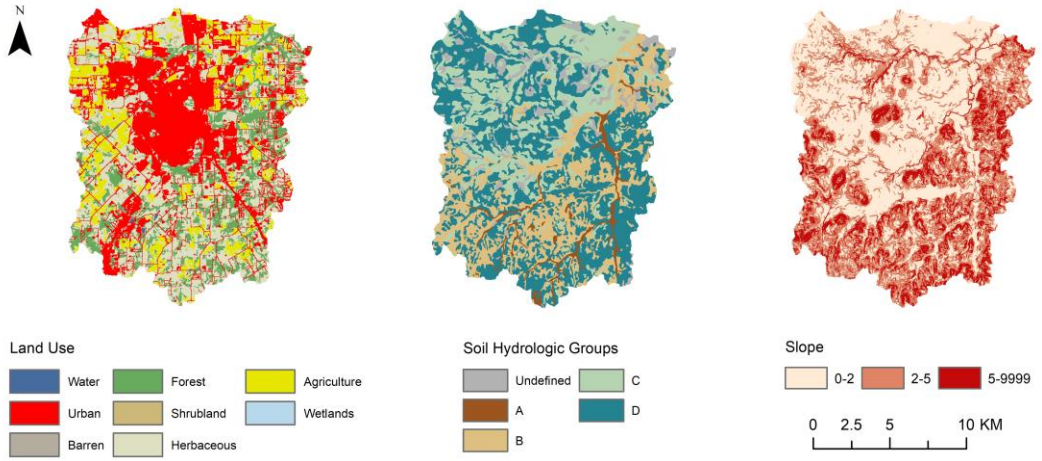

Figure 3. Land cover, soil hydrologic groups, and slope in the Village Creek watershed

The VC watershed climate is humid subtropical, with average annual temperatures range from 7.5℃ to 29.5℃ (Hoff, 2019). On average, the watershed receives about 907 mm of total precipitation annually (Hoff and Kipatrick, 2017a). However, in 2015 heavy storms well exceeded this average, bringing a record-breaking total annual precipitation of 1,600.3 mm. (Hoff, 2019; Hoff and Kipatrick, 2017a; NCTCOG, 2016). Specifically, April and May of 2015 had total monthly precipitation that drastically exceeded the average due to continuous storm events, resulting in extensive flood events and economic loss (Hoff, 2019; NCTCOG, 2016).

The watershed has experienced water quality problems, to the extent that the Texas Commission on Environmental Quality (TCEQ) classified the river segments (Segment ID 0828A) as "impaired." Since 2010, there have been elevated levels of *E. Coli* in various river segments of the watershed, with concentrations five times the standard set by TCEQ (Hoff and Kipatrick, 2017b). Potential sources of *E. coli* contamination include on-site sewage facilities (septic systems), livestock animals (cattle, sheep, goats, horses), wild deer populations, and domestic pets (cats, dogs) (Hoff and Kipatrick, 2017b; Hoff et al., 2018).

E. coli is the primary pollutant of concern for VC (EPA, 2017a) due to high levels exceeding the TCEQ standards of 126 CFU/100mL. Sources for *E. coli* are associated with septic systems and animal manure. Septic systems are located throughout the watershed, with an estimated 6,257 in the urban and rural areas (Hoff et al., 2018). As previously discussed, there are various reasons septic systems can fail and release the effluent into the waterbodies, with accumulating bacteria and nutrients. Systems over 25 to 30 years old have a higher risk of failure due to system age and lack of maintenance of these systems; however, these are more difficult to find due to the lack of permitting (EPA, 2005; Hoff et al., 2018). Septic system failure rates in Texas are

estimated to range between 10-15% and can result in the surfacing of effluent and contamination of surface and groundwater (U.S. EPA, 2002). Additionally, livestock and wild animals are other primary pollution source in this watershed. Specifically, stormflow can carry the manure from the animals into the neighboring waterbodies. These animals included in this study are cattle, sheep, goats, horses, and wild deer.

The water quality issues led to the development of the Village Creek – Lake Arlington Watershed Protection Plan (WPP). This WPP was implemented by the Trinity River Authority (TRA) to enhance the water quality in the watershed by identifying pollution sources, areas of concern and developing management strategies to eliminate the pollution. Given the watershed's location, urban growth trend, and current water issues, the VC watershed serves as an ideal peri-urban watershed to model *E. coli* and estimate the potential benefits of GI implementation.

Objectives

This study estimates the benefits of implementing green infrastructure on water quality, *specifically E. coli*, in the Village Creek watershed. The question is, how can Village Creek reduce *E. coli* concentrations below the required TCEQ standards of 126 CFU/100mL? Using a SWAT model to represent the VC watershed, simulations will test how GI practices may reduce *E. coli* concentrations. The specific objectives include:

1. Develop and calibrate a model of the VC watershed in SWAT to represent the current streamflow and *E. coli* conditions in the watershed. The calibrated model serves as a baseline scenario and will be used to compare other GI scenarios.
2. Simulate scenarios of GI practices implemented in urban areas targeting *E. coli* reductions. The results may highlight the urban areas that are most effective for GI implementation to reduce *E. coli* concentrations.
3. Analyze and compare the results from baseline and GI scenarios to understand the changes in *E. coli* concentrations. The results will estimate the usefulness of GI practices in the watershed.

Section III. Methods

To meet the objective of estimating the impact of urbanization on water quality (*E. coli*) in the VC watershed, the following three crucial steps were carried out: 1. Model Development, 2. Model Evaluation, and 3. Model Application/scenario testing. Model development (step 1) includes collecting and analyzing input data to develop a model of the VC watershed using SWAT. Model evaluation (step 2) involves assessing the

performance of the VC watershed model to estimate streamflow and *E. coli* through model sensitivity analysis, calibration, and validation. Initially, the model is run "as-is" without any manipulation to evaluate the initial performance and identify the model's sensitivity to the inputs and associated parameters. The sensitivity analysis test provides information on model behavior to understand the influence of model-related inputs and parameters on the outputs, as observed through various statistical calculations. An uncertainty analysis is used to test model error for understanding how the variability/uncertainty in model inputs may affect the confidence of the outputs. The model calibration process helps identify parameters along with their associated range of values to produce a good fit between the observed and modeled data over a given simulation period. Then, the model validation process is used to test the model's reliability by taking the calibrated model and running it for a different simulation period. In both calibration and validation periods, uncertainty analysis assesses the error or variability in the model performances. Model application (step 3) involves applying the model to answer the research question and running it under different scenarios. The scenarios in this research study include the implementation of the GI practices to estimated reductions in *E. coli* under those scenarios.

1. Model Development

Data Collection

Various types of data were collected to construct and drive the VC watershed model (Table 2). By inputting elevation data, the model was able to delineate the VC watershed, create stream networks, divide the watershed into multiple sub-basins, and derive slope classes along with the associated topographic and geometric information. The information from land use/land cover, soil, and slope data were used to generate unique combinations of land, soil, and slope classes in each subbasin, called Hydrologic Response Units (HRUs). Watershed climate data (daily temperature and precipitation) drove the VC watershed model. Daily streamflow data were used to evaluate model sensitivity and perform model calibration and validation by comparing it with the modeled streamflow. Sources of bacteria such as domestic and wild animals and sewer systems were used to represent *E. coli* concentrations in the watershed. Also, the observed *E. coli* data were used to train the model for *E. coli* estimation. The observed *E. coli* data was obtained from the Texas Commission on Environmental Quality (TCEQ) surface water quality monitoring (SWQM) program. *E. coli* samples were collected and analyzed primarily by Trinity River Authority (TRA) of Texas following the TCEQ

bacteriological sample collection procedure (TCEQ, 2012). Table 2 provides detailed information about these data.

Table 2. Data used to develop the Village Creek Watershed model. The source (and hyperlink), resolution/general description, and the period of the data are included.

Data Type	Source	Resolution/Description	Time Period
National Watershed Boundary Dataset	United States Geological Survey (USGS)	1:24,000	2016
Digital Elevation Model (DEM)	United States Geological Survey (USGS)	10 m (1/3 arc second)	2019
Land Use Land Cover (LULC) (CONUS)	National Land Cover Dataset (NLCD) – Multi Resolution Land Characteristics Consortium (MRLC)	30 m	2016
Soil – Tarrant and Johnson County	Soil Survey Geographic Database (SSURGO) – United States Department of Agriculture (USDA) Web Soil Survey	county level	2019
Climate Data – Precipitation (mm) Maximum Temperature (˚C) Minimum Temperature (˚C)	PRISM Climate Group – Northwest Alliance for Computational Science and Engineering, Oregon State University	Daily	January 1, 1981 – December 31, 2019
Streamflow Discharge (f^3/s)	USGS - Water Data Station: USGS 08048970: Village Creek at Everman, TX	Daily	January 1, 1990 – December 31, 2019
Water Quality *Escherichia coli (E. coli)*	Texas Commission on Environmental Quality (TCEQ)- Surface Water Quality Monitoring Station ID: 10786	48 samples collected at the TCEQ monitoring site ID 10786 and the USGS gauge 08048970	2011 - 2019
Septic System Locations	Trinity River Authority (TRA) Heather Firn, Watershed Scientist III at TRA of Texas Contact: firnha@trinityra.org	Several point locations within Johnson and Tarrant counties	Point Data Compiled in 2015
Domestic Agricultural Animal Populations (cattle, sheep/lamb, horses)	Census of Agriculture (USDA)	County level	2017, 2012, 2007

Cattle Stocking Rates	Jacklyn Jones (Tarrant County) and Justin Taylor Hale (Johnson County), Agriculture & Natural Resources Extension Agents, Texas Agri-life extensions, Contact: Jacklyn.Jones@ag.tamu.edu justin.Hale@ag.tamu.edu	County level	Contacted in 2020

Daily precipitation and temperature data were obtained from the PRISM Climate Group for five locations within the VC watershed (Fig. 2). These five stations cover the full extent of the watershed: station A in the North-West (NW) region, station B in the North-East (NE) region, station C in the South-West (SW) region, station D in South-East (SE) region, and station E in the middle (MID) region of the watershed (Fig. 2). Analysis of the daily temperature and precipitation data for the simulation period (2001 – 2019) provided insights into the varying climatic conditions (such as dry, wet, and average) of the VC watershed.

Analysis of temperatures at daily, monthly, and annual scales provided insights into the temperature trends in VC. The temperatures were consistent across the watershed, having similar daily temperature averages and ranges between stations. The annual temperatures did not vary, as the average minimum and maximum temperatures were consistent between 2001 and 2019. On a monthly scale, the watershed reaches its maximum temperatures in August, with a daily average of 29.3˚C (Fig. 4). From 2001 to 2019, the average of all stations is 18.7˚C ranging between a low of 9.0˚C and a high of 35.9˚C in the VC watershed.

Figure 4. Average daily temperature from all five stations on a monthly scale

The analysis of the cumulative annual precipitation at each station provided the spatial distribution of rainfall in the watershed (Fig. 5). The average yearly total precipitation in the watershed during the model simulation period (2001 – 2019) was 906.8 mm, with the lowest (434.7 mm) in 2005 and highest (1,600.3 mm) in 2015. Spatially, station D in the SE part of the watershed received the highest average precipitation between 2001 and 2019, followed by station C (SW), station A (NW), station E (MID), and station B (NE). The spatial pattern shows some precipitation gradient within the watershed with larger quantities in the southern and western regions and decreasing in the north-eastern region.

Figure 5. Cumulative annual precipitation for five stations in the Village Creek watershed

Additionally, the average daily precipitation per month was used to find the wetter and drier periods of the year (Fig. 6). May (3.62 mm) and October (3.36 mm) received the highest daily averages over the simulation period. While July (1.67 mm) and December (1.74 mm) tend to experience the lowest daily precipitation averages. May has the largest precipitation ranges, with minimum daily precipitation of 1.51 mm and a maximum of 13.29 mm per day. August has the lowest amount of rainfall, at 2.83 mm.

Figure 6. Average daily precipitation at monthly scale in the Village Creek watershed

Streamflow Measurement

The streamflow data, collected at the USGS gauging station (USGS 08048970) for the model simulation years (2001 to 2019), represents the observed streamflow conditions in the watershed. Evaluating this data served as a basis to assess the performance of the VC model for calibration and validation. For the watershed, streamflow ranged from <0.5 m^3/s to 179.96 m^3/s, with an average observed daily discharge of 1.3 m^3/s (Fig. 7). On a monthly scale, the highest average daily flow was in May with 2.93 m^3/s, followed by March with an average of 2.18 m^3/s. December and August had the lowest streamflow volumes, 0.36 m^3/s, and 0.70 m^3/s, respectively, owing to drier conditions in those months during the model simulation period.

Figure 7. Average daily streamflow for each month in the Village Creek Watershed.

The observed streamflow was partitioned between the baseflow and stormflow using the recursive digital filter method available in the Web-Based Hydrograph Analysis Tool (WHAT) (Lim et al., 2005) to gain valuable insights into the VC watershed hydrology. This method produced an important indicator, called baseflow index (BFI), which is the ratio of the baseflow to streamflow for the VC watershed (eq. 1).

$$b_k = [(1 - BFI_{max}) \times a \times b_{k-1} + (1 - a) \times BFI_{max} \times y_k] \div (1 - a \times BFI_{max}) \quad \textit{Equation 1}$$

Where, b_k is the baseflow at time step k, b_{k-1} is the baseflow at time step k-1, y_k is the total streamflow at time step k, BFI_{max} is the baseflow index which is the ratio of baseflow to the total streamflow, and a is the filter parameter value.

Analysis of the streamflow record between 2001 and 2019 estimated the baseflow index of 0.287; it means that about 28.7% of the streamflow in the VC watershed is comprised of baseflow (Fig. 8). The average observed streamflow, stormflow, and baseflow for the 2001 to 2019 period were 1.30 cm/s, 0.93 cm/s, and 0.37 cm/s, respectively. The highest streamflow was recorded in 2015, consistent with the above-normal precipitation (Fig. 8) (NCTCOG, 2016). The 2015 average streamflow was 3.55 m^3/s, with baseflow making up 26.3% (0.93 m^3/s) and the remaining flow consisting of stormflow (2.62 m^3/s). The second-highest year was 2007, in which the average streamflow, stormflow, and baseflow were 2.67 m^3/s, 1.81 m^3/s, and 0.86 m^3/s, respectively. These streamflow records also correlate with the precipitation data, where 2007 was the year with

the second-largest volume of cumulative precipitation. The lowest streamflow years were 2014 and 2013. In 2014, streamflow averaged about 0.25 m^3/s, with an average baseflow of 0.07 m^3/s and stormflow of 0.18 m^3/s.

Figure 8. Observed streamflow and the digital filter partitioned stormflow and baseflow in the Village Creek watershed

Water Quality Measurement

Observed *E. coli* data, the primary water quality concern for this research study, were obtained from Texas Commission on Environmental Quality (TCEQ). The stream gauge station, also the site for streamflow measurements, was the collection location of these data (Fig. 2). There were only 48 observations between 2011 and 2019, ranging from one to 13 records each year (Figure 9). The reported unit of measurement for *E. coli* was the Most Probable Number per 100 mL (MPN/100mL), equivalent to the statistical probability of the colony-forming units per 100mL (CFU/100mL).

Figure 9. Observed E. coli count for the water quality monitoring station 10786: Village Creek at Rendon Road

The TCEQ standard for *E. coli* is set to 126 CFU/ 100mL, and the average annual water quality measurements are above the standard for seven out of the ten years. Also, 24 out of 48 records exceeded the acceptable level between 2011 and 2019. The year with the highest *E. coli* concentrations was 2015, which is also the year with the highest streamflow discharge and average precipitation. There is a substantial decrease in the reported *E. coli* counts in 2017, 2018, and 2019 compared to the previous years (Fig. 9). According to Trinity River Authority representatives (Heather et al., personal communication, May 2021), there is no definite answer for this decline in *E. coli* concentrations; however, they provided two possible reasons. First, the decline was most likely due to a reduction in livestock activities, which would have limited the discharge of *E. coli* from their manure into the river networks. Secondly, there could have been potential repairs of broken or failed wastewater infrastructure in the watershed; however, no record of such activity is documented.

Model Development

The development of the VC watershed model included the following key steps: watershed delineation, hydrologic response unit (HRU) distribution, model input table creation, and model simulation. Watershed delineation used the DEM raster data to define the watershed boundary, an area of 232 km^2, create stream networks, divide the watershed into 21 sub-basins, and derive the associated stream and topographic information (Fig. 10). The application of a 5.5 km^2 threshold area limited the number of sub-basins to closely

mimic the number of HUC-12 sub-watersheds within the VC watershed. The USGS streamflow gauging station defined the location of the watershed outlet. The resulting subbasins ranged from 2 km^2 to 21 km^2, with an average area of 11 km^2.

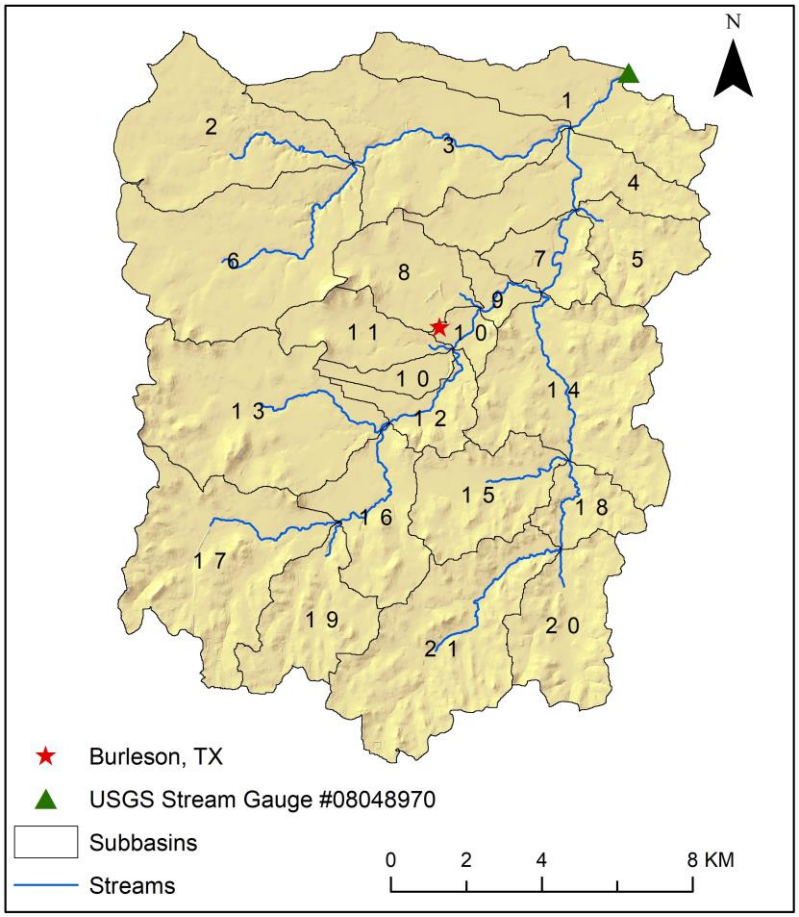

Figure 10. Study area map with the delineated subbasins with the DEM data

A hydrological response unit (HRU) is the smallest unit area within a watershed, consisting of unique combinations of land uses, soil types, and slope classes. According to the 2016 land use land cover data, 15 types of land uses are grouped into eight major categories (Fig. 3), of which rangeland (~35%) and urban areas (~34%) are dominant in the watershed, followed by other land uses. The SSURGO soil database of the VA watershed contained 1,791 unique soil types within four hydrologic soil groups as defined by map unit key (MUKEY). For this study, three slope classes divided the watershed: 0-2%, 2-5%, and >5%. Overlaying these land uses, soil types, and slope classes resulted in 7,579 HRUs. However, by applying a 5% threshold to all land cover types, except urban areas, and a 10% threshold to all soil and slope areas, the number of HRUs decreased to 835. These HRUs all had unique combinations of eight land uses, 51 MUKEY soil types, and three slope

classes. The exclusion of urban land classes from the 5% threshold included all urban areas to analyze the impacts of urbanization on *E. coli* in the VC watershed.

The model development stage included the creation of several input tables or model input databases. These tables consist of various model parameters with their associated values generated from the watershed topographic information, HRU distribution, and climate data. The climatic condition defined in the watershed used daily precipitation and temperature data from the five stations within the watershed (Fig. 2). These input tables store information about model parameters and hydrological processes related to evapotranspiration, and rainfall-runoff relationships to calculate the storage and routing of water, sediment, nutrients, and pathogens including *E. coli* in the watershed. In this project, the Penman-Monteith method (Eq. 2) (Monteith, 1965; Neitsch et al., 2011) was used to estimate potential evapotranspiration. This method requires solar radiation, air temperature, relative humidity, and wind speed to calculate the potential evapotranspiration of the watershed at daily time scale (Monteith, 1965). The solar radiation, relative humidity, and wind speed data used in the PET calculation were taken from the built-in SWAT weather database.

$$\lambda E = \frac{\Delta \times (H_{net} - G) + \rho_{air} \times c_p \times [e_z^o - e_z] \div r_a}{\Delta + \gamma \times (1 + r_c \div r_a)} \qquad \textit{Equation 2}$$

Where, λE is the latent heat flux density, E is the depth rate evaporation, Δ is the slope of saturation vapor pressure-temperature curve, H_{net} is net radiation, G is the heat flux density to the ground, ρ_{air} is air density, c_p is the specific heat at constant pressure, e_z^o is the saturation vapor pressure of air at height z, e_z is the water vapor pressure of air at height z, γ is the psychrometric constant, r_c is the plant canopy resistance, and r_a is the aerodynamic resistance.

The rainfall-runoff relationship is a way to estimate the volume of stormflow generated from a rainfall event (Neitsch et al., 2011). The Soil Conservation Service (SCS) Curve Number (CN) method was used to determine the rainfall-runoff relationship in the VC watershed model (Eq. 3) (Neitsch et al., 2011; Soil Conservation Service, 1972). CN values represent the infiltration and runoff conditions of an area, derived from combining the effects of soil, land use, slope, and hydrologic conditions. The SCS CN rainfall-runoff method utilizes the CN values of an area as the combinations of soil permeability, land use, and antecedent soil water conditions at the HRU level in the watershed (Neitsch et al., 2011). The retention parameter (Eq. 3) is the soil water content in relation to the soil water potential, which can change in response to varying soil types, land use and management, and slope (Neitsch et al., 2011).

$$Q_{surf} = \frac{(R_{day} - I_a)^2}{(R_{day} - I_a + S)}$$ *Equation 3*

Where Q_{surf} is the accumulated runoff or rainfall excess, R_{day} is the rainfall depth for the day, I_a is the initial abstractions, including surface storage, interception, and infiltration before runoff, and S is the retention parameter.

The variable storage method (Eq. 4) defined the method for water routing, which utilizes Manning's equation to calculate flow rate and velocity. Manning's equation (Eq. 5) calculates flow rates and velocity in an open channel. The calculation considers overland flow, slope, and Manning's roughness coefficient, or friction within the channel and applied to the water flow (Neitsch et al., 2011).

$$V_{in} - V_{out} = \Delta V_{stored}$$ *Equation 4*

Where V_{in} is the volume of inflow during the time step, V_{out} is the volume of outflow during the time step, ΔV_{stored} is the change in the volume of storage during the time step.

$$V_{ov} = \frac{q_{ov}^{0.4} \times slp^{0.3}}{n^{0.6}}$$ *Equation 5*

Where q_{ov} is the average overland flow rate (m^3/s^1), slp is the average slope (m/m), n is the Manning's roughness coefficient.

In SWAT, the bacterial module, developed by Sadeghi and Arnold (2002), is used to estimate pathogenic and non-pathogenic bacterial loads and concentrations in channels for two bacteria populations: persistent bacteria (e.g., *E. coli*) and less-persistent bacteria (e.g., fecal coliform) (Sadeghi and Arnold, 2002). In this study, only persistent bacteria (*E. coli*) are considered, and this group of bacteria has lower decay rates in natural conditions than less-persistent bacteria (Coffey et al., 2007). Estimating bacteria transport from the top 10 mm soil layer to the stream is a function of bacteria attached to sediments, runoff amount, soil bacteria contact, and bacteria enrichment ratio. The bacterial calculation in surface runoff used in SWAT (Eq. 6) is similar to the soluble phosphorous movement based on pesticide equations of Leonard and Wauchope (Knisel, 1980; Pierson et al., 2001)

$$Bact_{surf} = \frac{Bact_{sol} \times Q_{surf}}{\rho b \times depth \times BACTKDQ}$$ *Equation 6*

Where, $Bact_{surf}$ is the bacteria load in surface runoff (CFU/m^2), $Bact_{sol}$ is the bacteria count in the top 10 mm soil layer (CFU/m^2), Q_{surf} is the surface runoff volume (mm), ρb is the soil bulk density (mg/m^3),

and $BACTKDQ$ is the bacterial-soil partitioning coefficient (m^3/mg) which is expected to be independent of bacteria type, land-use and soil.

In the case of flowing water such as open channels or rivers or creeks, SWAT uses equation 7 to estimate bacteria concentration as below:

$$\Delta stream_{bact} = Bact_{surf} - Bact_{sed} + Direct_{input} - Decay_{stream} - Bact_{flow} \quad \textit{Equation 7}$$

Where $\Delta stream_{bact}$ is the change in bacteria loading in a day (CFU/m^2), $Bact_{surf}$ is bacterial loading in a soil solution (CFU/m^2), $Bact_{sed}$ is bacteria adsorbed to soil particles transported by surface runoff (cfu/m^2), $Direct_{input}$ is the bacterial loadings to rivers from sources such as wastewater treatment plants, $Decay_{stream}$ is the bacteria count decayed in a day (CFU/m^2), and $Bact_{flow}$ is the total count of bacteria carried by streamflow (CFU/m^2).

Because bacteria are considered to be dissolved pollutants, calculation of their concentration in water uses the first-order decay equation or Chick's law (Eq. 8) as proposed by Mancini (1978) and later modified by Moore et al. (1989).

$$C_t = C_0 \times e^{-k_{20} t_\theta^{(T-20)}} \quad \textit{Equation 8}$$

Where C_t is the concentration of bacteria in the river at the exposure time *t* in days, C_0 is the initial concentration of bacteria, k_{20} is the first order die-off rate at 20 ℃ per day, t_θ is the temperature adjustment factor denoted by the parameter *THBACT* in SWAT, and T is the ambient temperature in ℃. In SWAT, the first-order die-off rate for *E. coli* is set at 20 ℃ per day.

2. Model Evaluation

Model Simulation and Evaluation

The VC model was run for the 2001 – 2019 period using the processes mentioned above and SWAT default model parameter values. Then, the modeled streamflow at the watershed outlet was compared with the observed streamflow providing the model's initial performance before model calibration. An analysis of four statistical matrices, comparing the observed and modeled streamflow, showed the model's performance for simulating the observed VC conditions: average streamflow, Percent Bias (PBIAS), Coefficient of Determination (R^2), Nash-Sutcliffe Efficiency (NS), and Kling-Gupta Efficiency (KGE).

Percent Bias (PBIAS) measures the average likelihood that the modeled outputs are larger or smaller than observed measurements (Eq. 9). The PBIAS of zero is an optimal value with low-magnitude values

indicating accurate model simulation. If PBIAS is less than zero, then the model is overestimating and if it is greater than zero, the model is underestimating.

$$PBIAS = 100 \times \frac{\sum_{i=1}^{n}(Q_o - Q_s)_i}{\sum_{i=1}^{n} Q_{o,i}} \quad \textit{Equation 9}$$

Where Q is the discharge, O stands for observed, s stands for modeled, and i is the number of ith measured or modeled data.

Coefficient of Determination (R^2) explains how well the modeled and observed streamflow fall along a line of best fit (Eq. 10). R^2 values range from zero to one, with values closer to one indicating a better goodness of fit.

$$R^2 = \frac{\left[\sum_i \left(Q_{o,i} - \overline{Q_o}\right)\left(Q_{s,i} - \overline{Q_s}\right)\right]^2}{\sum_i \left(Q_{o,i} - \overline{Q_o}\right)^2 \left(Q_{s,i} - \overline{Q_s}\right)^2} \quad \textit{Equation 10}$$

Where Q is the discharge, O stands for observed, s stands for modeled, and i is the number of ith measured or modeled data.

Nash-Sutcliffe Efficiency (NS) evaluates the prediction strength and reliability of a model and describes the model's accuracy (Eq. 11). NS value ranges between negative infinity to 1, with NS = 1 indicating a perfect match between the observed and modeled data. If NS is equal to zero, then it means that the model predictions are as accurate as the mean of the observed data (also known as no-knowledge model), and anything less than zero indicates that the model is a no-knowledge model.

$$NS = 1 - \frac{\sum_i (Q_o - Q_s)_i^2}{\sum_i \left(Q_{o,i} - \overline{Q_o}\right)^2} \quad \textit{Equation 11}$$

Where Q is the discharge, O stands for observed, s stands for modeled, and i is the number of ith measured or modeled data.

Kling-Gupta Efficiency (KGE) is an alternative to NSE to measure the agreement between the observed and modeled data (Eq. 12) (Knoben et al., 2019). KGE values range from -α to 1, where KGE=1 shows a perfect agreement, and the closer KGE is to 1, there is a stronger agreement between the two datasets. (Knoben et al., 2019).

$$KGE = 1 - \sqrt{(r-1)^2 + (\alpha - 1)^2 + (\beta - 1)^2} \quad \textit{Equation 12}$$

$$\alpha = \frac{\sigma_s}{\sigma_o}, \beta = \frac{\mu_s}{\mu_o}$$

Where, σ_s and σ_o are the standard deviations of modeled and observed data, μ_s and μ_o are the average simulated/modeled and observed data, *r* is the linear correlation between observed and modeled results, α is the flow variability error, and *s* is the bias.

Model Simulation: Streamflow Pre-Calibration

The streamflow simulation was from January 1, 2001, to December 31, 2019, with a 10-year warm-up period. A "warm-up period" allows the model to cycle through hydrologic processes properly, making the data more stable before comparing it to observed data. The model output does not include the data from the warm-up period. The performance of the model in terms of streamflow estimates was conducted for three periods: the entire simulation period (2001 – 2019), the first ten years (2001 – 2010), and the later nine years (2011 – 2019). The 2011 – 2019 period was used for model calibration, and 2001 – 2010 was used for model validation.

Comparisons between the observed and modeled results indicated a good model performance, with $R^2 \geq 0.65$ and NSE ≥ 0.59, in predicting the Village Creek watershed streamflow (table 3). However, for the 2001-2019 period, the model overestimated streamflow by 39.2%, with the modeled average streamflow of 1.81 m^3/s, compared to the observed 1.30 m^3/s. It was a good starting point for an un-calibrated model. The VC model is better than a no-knowledge model with a good prediction strength (NSE > 0). The positive linear relationship with $R^2 \geq 0.65$, the pre-calibrated model, could explain 65% of the observed streamflow.

Table 3. Statistical comparison between pre-calibrated model and observed streamflow.

Time Period	R^2	NSE	KGE	Percent Bias	BFI	Avg. Modeled Discharge	Avg. Observed Discharge
2001-2019	0.71	0.65	0.66	39.2%	0.328 (0.287)	1.81 m^3/s	1.30 m^3/s
2001-2010	0.65	0.59	0.71	27.2%	0.322 (0.285)	1.73 m^3/s	1.36 m^3/s
2011-2019	0.78	0.71	0.73	55.7%	0.335 (0.290)	1.90 m^3/s	1.22 m^3/s

Note: values in parenthesis indicate BFI for observed streamflow

For the 2001 – 2019 model simulation period, the modeled streamflow had a BFI of 0.328 compared to 0.287 for the observed streamflow for the same period. The uncalibrated model seemed to systematically over-predict both baseflow and stormflow in the calibration (2011-2019) and validation periods (2001-2010). (Figure 11).

Figure 11. The USGS Observed and SWAT modeled stormflow and baseflow for the pre-calibrated model, during the 2001 – 2019 period

Model Calibration and Validation

Water Quantity: Streamflow

Model calibration is the process of adjusting values of model parameters to improve the model's predicting strength being within a specific range of uncertainty. This process compares the observed data to the modeled data, allowing us to identify critical parameters, assign parameter values, and adjust the parameters to fine-tune the model.

SWAT-CUP, a model calibrator (Abbaspour, 2015), was used to calibrate the VC watershed model. SWAT-CUP includes an algorithm called SWAT Parameter Estimation (SPE) for model calibration, validation, sensitivity, and uncertainty analysis. SPE investigates the origin of uncertainties for all input variables, parameters, and measured data to determine the uniform distribution or range of parameter uncertainties through several iterations (Abbaspour, 2015). Each iteration of the SPE identifies a better performing output (e.g., streamflow) by highlighting all parameter and variable uncertainties to find a range of "good solutions" that captures the measured streamflow values (Abbaspour et al., 2015). SWAT-CUP uses a Latin hypercube sampling method which randomly selects parameter values and assigns them in each iteration to develop a range of output uncertainties, which serves as the 95% probability distribution. It is calculated from the 2.5% to 97.5% percentiles of the output variable distribution, serving as the 95% prediction uncertainty (95PPU)

"envelope" or bracket (Abbaspour, 2015). The 95PPU is a random calibration technique that generates an envelope of output variables using the range of parameter values (Lim et al., 2005). Ideally, the model with a narrow envelope size captures a large percentage of the measured data (e.g., streamflow), meaning that the model has a low prediction uncertainty while also capturing a large portion of the measured data (Abbaspour, 2015).

To evaluate the 95PPU of the model, two statistical measures, p-factor, and r-factor, are used in SWAT-CUP. The p-factor represents the amount of observed data that falls within the 95PPU envelope (Abbaspour, 2015; Abbaspour et al., 2015). The p-factor values range from 0 to 1, where a p-factor equal to 1 implies that 100% of observed values fall within 95PPU. The r-factor is the average width (thickness) of the 95PPU envelope, or range of uncertainty, with values ranging from 0 to infinity (Abbaspour et al., 2015). Since r-factor demonstrates a degree of uncertainty, it is ideal to have a smaller value. By running several SPE iterations, it is expected that parameter ranges condense or become narrower, resulting in a lower model uncertainty by taking in the highest performing results from the previous cycle and eliminating parameter uncertainty.

The SPE method includes both single and multiple objective functions to maximize parameter values and obtain specific goals for observed measurements and modeled outputs (Abbaspour, 2015). Calibration for the VC watershed model used a multi-objective function (Eq. 13), including PBIAS, R^2, bR^2, RSR, NS, and KGE.

$$g = (w_3 R^2 + w_5 NS + w_6 bR^2 + w_9 KGE) - [w_8 |PBIAS| + w_{10} RSR] \quad \textit{Equation 13}$$

Where, g is the goal parameter value and w is the weight the objective function holds.

bR^2 (Eq. 14) is a calculation that accounts for the variances between the observed and modeled discharges, based on the "magnitude of two signals", "b" , and dynamics, R^2 (Abbaspour, 2015).

$$bR^2 = \begin{cases} |b| R^2 & if \quad |b| \leq 1 \\ |b|^{-1} R^2 & if \quad |b| > 1 \end{cases} \quad \textit{Equation 14}$$

Where, R^2 is the coefficient of determination (Eq. 10), and b is the coefficient of regression line between observed and modeled results.

RSR (Eq. 15) is an objective function used to show the relationship between modeled and observed data. When evaluating RSR results, values can range from 0 to a very large; however, lower values are desired to show good model performance.

$$RSR = \frac{\sqrt{\sum_{i=1}^{n}(Q_o - Q_s)_i^2}}{\sqrt{\sum_{i=1}^{n}(Q_{o,i} - \overline{Q}_o)^2}}$$ *Equation 15*

Where, Q is the discharge (m^3/s), o stands for the observe discharge, and s stands for the simulated/modeled discharge.

The model was run for 1,000 simulations with 22 parameters (Table 4). Global sensitivity analysis identified the most sensitive parameters by evaluating parameter values to see how parameter values influence the objective functions and model outputs. A t-test measured the sensitivity of each significant parameter, found through the t-stat and p-value (Abbaspour, 2015). A parameter is considered more sensitive when the t-stat value is larger and the p-value is smaller (Abbaspour, 2015). Therefore, the calibrated parameters were those with lower p-values, usually less than 0.5. Then the model was run for 1,000 simulations to calibrate it using the most sensitive parameters.

Table 4. Model parameters used for the Village Creek watershed model sensitivity analysis. The parameters are ordered from the least sensitive (lower t-stat and higher p-value) to the most sensitive (higher t-stat and lower p-value).

SN	Parameter Name	t-Stat	P-Value
1	r__OV_N.hru	0.0415	0.9669
2	v__CH_N2.rte	-0.2099	0.8338
3	v__SURLAG.hru	-0.2740	0.7842
4	v__REVAPMN.gw	-0.3168	0.7514
5	v__DEEPST.gw	-0.3297	0.7417
6	v__CH_K1.sub	0.3609	0.7182
7	v__ALPHA_BNK.rte	-0.3929	0.6945
8	v__ALPHA_BF.gw	0.6776	0.4982
9	r__HRU_SLP.hru	0.8361	0.4033
10	v__GW_REVAP.gw	0.8977	0.3695
11	v__GW_DELAY.gw	-1.8278	0.0679
12	r__SLSUBBSN.hru	-2.1811	0.0294
13	v__CH_N1.sub	-2.1936	0.0285
14	v__SHALLST.gw	-2.6798	0.0075
15	v__GWQMN.gw	3.2381	0.0012
16	v__RCHRG_DP.gw	-3.5232	0.0004
17	v__EPCO.hru	3.6426	0.0003
18	v__CH_K2.rte	4.2540	0.0000
19	v__DEP_IMP.hru	5.8825	0.0000
20	r__SOL_AWC().sol	6.4067	0.0000
21	r__CN2.mgt	-17.5234	0.0000
22	v__ESCO.hru	-28.7202	0.0000

Twelve most sensitive parameters with a p-value ≤ 0.1 (Table 5) were deemed highly sensitive to model performance and therefore were used for model calibration. These parameters influence the HRUs, groundwater, subbasin, soil, and management input files.

Table 5. Parameters used to calibrate and validate the Village Creek watershed model along with their value ranges and fitted values

Parameter	**Min. Value**	**Max. Value**	**Fitted Value**
v__ESCO	0.50	1.0	0.68
v__EPCO	0.50	1.0	0.37
v__DEP_IMP	0.00	6000	1323
r__ SLSUBBSN	-0.25	0.25	-0.055
r__CH_N1	0.00	0.15	0.02
v__GW_DELAY	1	100	49
v__SHALLST	0	5000	1712
v__GWQMN	0	6000	3831
v__RCHRG_DP	0.01	0.9	0.18
v__CH_K2	0.025	10	4.95
r__SOL_AWC	-0.1	0.1	-0.0005
r__CN2	-0.2	0.1	-0.12

Note: “v” refers to replacement, and “r” refers to multiplication

Soil uptake compensation factor (ESCO), plant uptake compensation factor (EPCO), average slope length (SLSUBBSN), and depth to impervious layer in the soil profile (DEP_IMP) were the sensitive parameters from the HRU input file. ESCO defines the soil depth range for soil evaporation demands of the capillary water within the pores and cracks in the soil (Neitsch et al., 2011). ESCO was slightly lowered (default = 0.95), meaning there is less evaporation in the upper levels of the soil and more evaporated from lower levels of the soil, which decreases the modeled streamflow of an area. DEP_IMP defines the depth at the impervious layer within the soil profile, which can influence the amount of ponding water above the impervious layer (Neitsch et al., 2011).

SWAT includes a shallow, unconfined aquifer system and a deep, confined aquifer. The shallow aquifer contributes to the return flow of streams in the watershed, where the deep aquifer does not. The groundwater (.gw) input file adjusts parameters related to the flow of water in aquifers. The calibrated parameters in this input file were the deep aquifer percolation fraction (RCHRG_DP), the threshold depth of water in the shallow aquifer (GWQMN), the groundwater delay time (GW_DELAY), and the initial depth of water in the shallow aquifer (SHALLST). RCHRG_DP is the recharge of the deep aquifer through percolation.

The GWQMN parameter determines the water depth value in the shallow aquifer, allowing for groundwater flow to occur. GW_DELAY, measured in the number of days, defines the lag time of water recharging the shallow aquifer from the soil profile. A higher parameter value means a longer lag time for groundwater to reach the aquifer.

The subbasin general input file includes parameters that define the unique features in the subbasin (Neitsch et al., 2011). The Mannings "n" roughness coefficient value for the tributary channel (denoted byCH_N1 in SWAT) was the sensitive parameter in this input file. Manning's coefficient defines the roughness or friction experienced by the river networks and impacts water flow in the channels. Increasing the value of this parameter decreases the velocity due to a more considerable amount of resistance to flow. For example, for natural streams with few trees, stones, or brush, CH_N1 value ranges between 0.025 to 0.065, while for the excavated straight and uniform channel, its value ranges between 0.016 to 0.033. In SWAT, the default value is 0.014. The calibrated value of 0.02 suggests that the channel in the VC watershed is a natural stream with few trees, stones, or brush.

The soil input file contains a list of parameters representing the soil's physical and chemical characteristics and its interaction with water and air at different layers in each HRU. The calibrating of the parameter, SOL_AWC, adjusts the available water capacity of soil layers. A soil's available water capacity is the amount of water stored in the soil available for plants to use; therefore, changing the value of this parameter changes the total water stored in soils throughout the watershed.

The main channel input file (.rte) includes parameters that represent physical characteristics of stream networks in the watershed, allowing for the model to run the physical processes relating to the movement of water, sediment, nutrient, and pesticide in the main channel (Neitsch et al., 2011). For the VC watershed model, the most sensitive parameter is related to the effective hydraulic conductivity in the main channel alluvium as denoted by CH_K2 in SWAT. This parameter controls the contribution of water from the reach or channel to groundwater (i.e., losing stream), from the groundwater system to the channel (i.e., gaining stream), and simultaneous movement of water between the channel and groundwater (i.e., flow-through stream). With the calibrated value of 4.95 mm/hour, the channel is characterized by a consolidated bed material with high silt-clay content, allowing a low to moderate water loss into the soil surface or groundwater (Neitsch et al., 2011).

Finally, the HRU management file describes the land and water management practices in the watershed. In this file, the calibrated parameter is the initial SCS runoff curve number for moisture condition

(II) (CN2). This process changes CN values for the whole watershed and down to the individual HRUs. The calibrated parameter reduces the CN value by 12% of the original CN value, providing a lower runoff potential.

After the model calibration was completed, the model was executed under a different period (2001 – 2010) for another set of 1000 simulations using the same parameters and their associated value ranges as in the model calibration period. This process allowed the analysis of the model's performance under two different periods with the same parameters and associated values.

Water Quality: *E. coli*

In addition to streamflow, the model was calibrated for water quality, i.e., *E. coli*, after adopting the bacteria simulation module by Jeong et al. (2019). The source code of the SWAT 2012 ver. 670 was modified to include *E. coli* related input at the HRU level and the routing and calculation of *E. coli*, allowing for the simulation of *E. coli* concentrations, transport, and loadings in the natural conditions and under different scenarios of GI implementation. According to the TCEQ, *E. coli* concentrations are the main water quality concern for the VC watershed. Therefore, the model calibration for *E. coli* used the sporadic measured data obtained from TCEQ. In this study, model inputs defined potential *E. coli* sources at the HRU level, such as septic systems (OSSF) and manure from cattle, goats, sheep/lambs, horses/ponies, and deer.

OSSF failures can release *E. coli* and N, P, and solids into surrounding areas, including waterbodies. The OSSF location data were obtained from the Trinity River Authority (Hoff, 2019). For methods used in collecting and developing OSSF data, refer to page 97 of the Village Creek Watershed Protection Plan (Hoff, 2019). There were 6,257 septic locations in the VC watershed, with 2,147 permitted systems, and the rest were unpermitted systems. The OSSF locations installed before 1989 do not have permits and have higher failure risks due to the lack of inspection. The model reads the septic systems at the HRU level. For this, the OSSF locations were overlayed in ArcMap with the SWAT generated HRU polygons. This resulted into an overlap of 3,686 OSSF locations with the SWAT HRUs.

According to the U.S. EPA, Texas's average OSSF failure rate is 10-15% (U.S. EPA, 2002). This study used a 12% OSSF failure rate to estimate *E. coli* concentrations generated from OSSFs in each HRUs. An individual household with an OSSF has an estimated average of 3.46 people, with an effluent rate of 0.227 liters/day/person. The study assumed that OSSF effluent contains approximately 5,000 CFU/100mL fecal coliform, equivalent to 1.58 CFU/100 mL *E. coli*. This analysis allowed for the estimation of total E. coli per

HRU. Furthermore, Dr. Jeong edited the SWAT source code to include the amount of E. coli discharge from each of the HRUs.

Another major contribution to *E. coli* pollution was manure generated from domestic and wild animals (Table 6). For this, analyzing cattle information for the VC watershed included collecting animal stocking rates per county for cattle, as obtained from the Texas Agricultural Life Extension for Johnson County and Tarrant County. Stocking rates represent the average animal unit (AU) per acre in a county, where one animal unit represents a 1,000-pound (lb) animal. For Tarrant County, stocking rates ranged from 1 AU per 10-12 acres for native grass and 1 AU per 8-10 acres for improved grass. Therefore, the stocking rate used for Tarrant Count was 1 AU per 10 acres (1 AU per ~4 hectares (HA)). For Johnson County, based on the communication with the county specialist, the "ideal" stocking rates ranged from 1 AU per 5-7 acres, but "less than ideal" conditions ranged to 1 AU per 7-10 acres. Therefore, the stocking rate in Johnson County was 1 AU per 7 acres (1AU per ~3 HA). For other animals (goats, sheep/lamb, and horses/ponies), the stocking rate was calculated by averaging total populations from 2007, 2012, and 2017 USDA Census of Agriculture and dividing by the total area of rangeland in each county. The stocking rate of 59 AU per 1,000 acres (59AU per ~24 HA) was used for deer, as reported by the Texas Landowner Association.

Table 6. Animal stocking rates and land cover used in total manure calculations

Animal of Concern	Stocking Rate (AU/HA)	Type and percentage of land cover within the watershed that falls in each county
Tarrant County (Subbasin 1-7)		
Cattle	0.2471	Range (33.5%)
Goats	0.0086	
Sheep/Lamb	0.0083	
Horses/Ponies	0.0178	
Deer	0.1458	Forest (8.8%)
Johnson County (Subbasin 8-21)		
Cattle	0.3530	Range (38.3%)
Goats	0.0352	
Sheep/Lamb	0.0138	
Horses/Ponies	0.0328	
Deer	0.1458	Forest (19.7%)

The total *E. coli* from animal manure was input into the model as grazing operations within the management file. The grazing operations in SWAT simulate animals grazing in the pasture or rangelands. For the model to simulate these operations, it must have the time of year and the length of the grazing period. Based on the email correspondence with Jacklyn Jones at Tarrant County Texas Agricultural Life Extension (December 2020), cool-season grazing occurs from late October to middle/late March, and warm seasons occur from April to September/October in Tarrant County. For Johnson County, according to Justin Hale at Johnson County (December 2020), cool-season grazing starts in November and ends in March, where warm-season occurs in the middle/late April and ends in October. Therefore, for the VC watershed model, grazing periods were assumed to take place throughout the year.

Additionally, the grazing operations require the amount of manure produced per day from each animal. Therefore, manure calculations from cattle, goats, sheep/lamb, and horses/ponies were applied to range HRUs, while the manure production from deer was applied to forest HRUs. Calculating the total manure produced by these animals used the county stocking rate and the dry manure production (equation 16). The average cattle manure production from one AU is 26.8 kg (59.1lb) per day, and 15% (4.02 kg/AU) is considered to be dry manure (USDA). This process was replicated for all other animals and their stocking rates (Table 6). The average manure dropped from goats, sheep/lamb, horses/ponies, and deer was 2.63 kg/AU, making their total dry manure 0.395 kg/day (Barker and Walls, 2002). These calculations provided the total manure dropped from each animal per HRU and were used to estimate the total manure for each sub-basin.

$$\text{Total Manure}\left(\frac{kg}{HA}\right) = \text{County Stocking Rate}\left(\frac{AU}{HA}\right) * \text{Dry Manure Prodution}\left(\frac{kg}{AU}\right) \qquad \textit{Equation 16}$$

Where the dry manure production is equal to 85% of the total manure produced. The average total manure produced for cattle is 26.8 kg/AU and for other animals including, goat, sheep/lamb, horse/pony, and deer is 2.63 kg/AU.

Model Simulation: E. coli Pre-Calibration

Using the *E. coli* loadings from various sources, the model simulated *E. coli* concentrations in VC. The simulated *E. coli* concentrations were 69.3% lower than the observed data (Table 7). It could be due to the lack of adequate input data (e.g., not accounting for all the sources of *E. coli*) and minimal *E. coli* observations available for comparison.

Table 7. Comparison of *E. coli* between observed and modeled before calibration

Time Period	Percent Bias	Geomean observed *E. Coli*	Geomean modeled *E. coli*
2011-2019	-69.3%	327.8 CFU/100 mL	100.8 CFU/100 mL

Then, the VC model was calibrated to optimize *E. coli* estimation using percent bias (eq. 9) and the geometric mean (geomean) (eq. 17). Finding the geomean shows the central tendency of two datasets by finding the product of the values. The geomean is frequently used in water quality monitoring, and an accurate measurement requires at least 20 measurements over seven years (Hoff, 2019). *E. coli* data was not regularly monitored; there were only 48 *E. coli* records over nine years, and only taking the arithmetic average would misrepresent the water quality condition. The geomean finds the performance results of the modeled data compared to the observed *E. coli* values.

$$\left(\prod_{i=1}^{N} x_i\right)^{1/N} = \sqrt[n]{x_1 \times x_2 \times x_3 \dots \dots x_n} \qquad \textit{Equation 17}$$

Where, Π is the geometric mean, n is the number of values in the dataset, and x_i is the values in the dataset.

Model Calibration: E. coli

The VC model was calibrated both manually and automatically using SWAT-CUP to estimate *E. coli* concentrations in the VC watershed by modifying values of ten parameters (Table 8) that are considered to influence bacteria estimation in SWAT. These parameters are in the SWAT basin (.bsn) input file. There are two types of bacteria in SWAT that can be modeled in SWAT, persistent and less persistent bacteria (Neitsch et al., 2011). Persistent bacteria have low decay rates and include *E. coli* and various pathogens, while less persistent bacteria, like fecal coliforms, have higher decay rates (Iqbal and Hofstra, 2019).

Table 8. A list of parameters used for E. coli calibration along with their calibrated values in the Village Creek watershed

Parameter	Definition	Pre-Calibration Value	Value Range	Fitted Value
BACTKDQ	Bacteria soil portioning coefficient (m^3/Mg)	125	0 - 500	2.43
THBACT	Temperature adjustment factor for bacteria die-off/growth (°C)	1.41	0 - 10	1.11
WDPQ	Die-off factor for persistent bacteria in the soil solution at 20˚C (per day)	0.11317	0 - 1	0.68
WGPQ	Growth factor for persistent bacteria in soil solution at 20˚C (per day)	0.11	0 - 1	0.44

WDPS	Die-off factor for persistent bacteria absorbed to soil particles at 20˚C (per day)	0	0 – 1	0.22
WGPS	Growth factor for persistent bacteria absorbed to soil particles 20˚C (per day)	0	0 - 1	0.67
WOF_P	Wash-off fraction for persistent bacteria	0	0 – 1	0.7
BACTMX	Bacteria percolation coefficient ($10m^3/mg$)	10	0 – 10	0.25
BACT_SWF	Fraction of manure applied to land areas that has active colony forming units	0.55	0.01 – 0.5	0.44
BACTMINP	Minimum daily bacteria loss for persistent bacteria (CFU/m^2)	0	0 – 10	5.75

The die-off and growth factors control the rates of reduction and production of *E. coli*. The parameters that control these factors include WDPQ, WGPQ, WDPS, WGPS, and BACTMINP used in the model calibration. WDPQ and WGPQ show the die-off and growth factors for persistent bacteria in the soil. Increasing the die-off factor resulted in a lower average of *E. coli* concentrations. WDPS and WGPS are the die-off and growth factor parameters for the persistent bacteria absorbed by the soil particles. Lastly, the die-off factor for persistent bacteria found in moving water (WDPRCH) was slightly sensitive in calibration.

BACTKDQ determines the total count of bacteria that is transported in stormflow (Iqbal and Hofstra, 2019; Neitsch et al., 2011). The default value is set to 175; however, it usually ranges from 0 to 500. Calibration reduced the default value to 2.4, where lowering the value of this parameter results in a larger concentration of *E. coli* units being transported via stormflow because less was retained by the soil (Parajuli, 2007). The temperature adjustment factor (THBACT) influences the die-off and growth rates at a given temperature. The default value given is 1.07; however, it can range from 0 to 10. Based on calibration, when the value of this parameter increases, this caused a decrease in *E. coli* concentrations. The wash-off fraction for persistent bacteria (WOF_P) calculates the number of bacteria on vegetation (foliage) that is washed off during a rainfall event (Neitsch et al., 2011). This parameter was not very sensitive to the model and did not significantly affect the *E. coli* outputs for the model. The bacteria percolation coefficient (BACTMX) is the ratio between bacteria in the soil surface and the amount that percolates in the soil surface (Neitsch et al., 2011). During calibration, the lowering of this values resulted in a decreased concentration of *E. coli*. BACT_SWF controls amount of active colony forming units on manure applied to land areas. Calibration showed that this parameter did not have a major influence on the model; however, when there was a decrease in the value, this resulted in a slight

decrease in average *E. coli* concentrations. Not all parameters were equally sensitive to the transport and concentration of *E. coli* in the VC watershed. Based on the global sensitivity analysis, BACTMINP, BACTMX, WGPS, THBACT and BACTKDQ were the five most sensitive parameters as indicated by p-values < 0.2 (Table 9) in the VC watershed.

Table 9. A list of parameters and their sensitivities to E. coli in the Village Creek watershed

Parameters	**t-Stat**	**p-Value**
WOF_P	-0.2506	0.8078
BACT_SWF	0.3065	0.7662
WDPQ	-0.3537	0.7317
WDPS	0.9740	0.3555
WGPQ	-1.0583	0.3175
BACTKDQ	-1.4603	0.1782
THBACT	1.8769	0.0933
WGPS	-2.1140	0.0637
BACTMX	-2.6034	0.0286
BACTMINP	2.8091	0.0204

3. Model Simulation and Application

The calibrated VC watershed model is assumed to estimate the impact of GI practices in controlling *E. coli* concentrations and transport. SWAT uses a fixed BMP operations utility to simulate GI practices allowing modelers to operate several scheduled management operations (.ops) (Neitsch et al., 2011). Of the several management operations, including terracing, tile drainage, contouring, filter strips, strip cropping, fire, grassed waterways, plant parameter, and residue management available in SWAT, the generic conservation practices are used as a fixed BMP operation to control sediment, nutrient, and bacteria outputs. The generic conservation practices allow implementing dozens of GI practices, also called urban BMPs, each with unique removal efficiencies for N, P, sediments, and bacteria. See the SWAT theoretical documentation for a list of all available generic conservation practices (page 497-500) (Neitsch et al., 2011). Table 10 provides a list of GI practices,

along with their removal efficiencies for bacteria. These removal efficiencies range from 40% to 90%, based on the review by Tetra Tech and NCTCOG (NCTCOG, 2021; Neitsch et al., 2011).

Table 10. A list of urban management operations along with their bacteria removal efficiencies available in SWAT

GI Practice	Reported Bacteria Reduction (%)
Alum Treatment	90
Dry Detention	70
Organic Filter	50
Planter Boxes	50
Sand Filters	40
Underground Sand Filters	40
Downspout Drywell	90
Infiltration Trench	90
Soakage Trench	90
Storm Water Ponds	70
Storm Water Wetlands	70
Submerged Gravel Wetlands	70

This research study tested a total of seven GI scenarios: scenarios 1 – 5 with a bacteria removal efficiency of 70% and scenarios 6 – 7 with a bacteria removal efficiency of 90%. These scenarios represent the placement of GIs on urban lands only represented by 472 HRUs in the VC watershed (Table 11). The period for the scenarios was 2011 – 2019, consistent with the period of model calibration for flow and bacteria.

Table 11. A list of green infrastructure (GI) scenarios implemented in the Village Creek watershed

Scenario	Bacteria Removal Efficiency	Land Cover	Slope class	Number of HRUs	Total Area (HA)	Percent area of the watershed
0. Baseline	No GI	Entire watershed				
1. U-70	70%	All urban	0 – 2%, 2 – 5%, and >5%	472	7,911	32.8%
2. U-HD	70%	Urban – High Density	0 – 2%, 2 – 5%, and >5%	130	1,708	7.4%

3. U-MD	70%	Urban – Medium Density	0 – 2%, 2 – 5%, and >5%	114	2,906	12.5%
4. U-LD	70%	Urban – Low Density	0 – 2%, 2 – 5%, and >5%	120	2,816	12.2%
5. U-I	70%	Urban – Industrial	0 – 2%, 2 – 5%, and >5%	108	481	2.1%
6. U-90	90%	All urban land	0 – 2%, 2 – 5%, and >5%	472	7,911	32.8%
7. U-HD-90	90%	Urban – Industrial	0 – 2%, 2 – 5%, and >5%	130	1708	7.4%

Scenarios 1 and 6 simulated the effects of GI implementation on all urban land covers to estimate its ability to reduce bacteria concentrations in the VC watershed (Table 11). Then, an additional five scenarios were tested to assess the removal efficacies of GI scenarios at locations of different urban intensities. Comparing the scenario results with the baseline *E. coli* allowed for evaluating the effectiveness of GI scenarios (percent reduction of *E. coli*) in the VC watershed. These results could provide insights on the suitability and effectiveness of different urban land uses for GI implementation based on their efficiencies.

Section IV. Results

Model Calibration and Validation

Water Quantity: Streamflow

The model was calibrated for daily streamflow in SWAT-CUP for the 2011 – 2019 period by modifying parameter values listed in Table 5 and comparing the modeled streamflow with the observation. Table 12 shows the SPE results and model performance for simulating streamflow for the calibration and validation periods. The SPE results showed that the model has a low prediction uncertainty (r-factor = 0.29) and can estimate about 72% of the observed streamflow without uncertainty (p-factor = 0.72). The model calibration showed a strong model performance as indicated by higher values of R^2= 0.85, NSE = 0.83, bR^2 = 0.81 and KGE = 0.90, and lower values of RSR = 0.41 and PBIAS = 0.2% in estimating the VC watershed streamflow.

The R^2 value of 0.85 was an improvement from the pre-calibrated value of 0.78. The model under-predicted by 0.2%, which is much improved compared to the pre-calibrated model overestimation of 55% (Table 12).

Table 12. Streamflow calibration and validation statistics for the Village Creek watershed

Results	p-factor	r-factor	R^2	NSE	bR^2	KGE	Percent Bias (%)	RSR	BFI	Avg. Modeled Discharge (m^3/s)
Calibration 2011-2019	0.72	0.29	0.85	0.83	0.81	0.90	0.2%	0.41	0.261 (0.287)	1.22 (1.23)
Validation 2001-2010	0.62	0.30	0.68	0.64	0.58	0.82	0.1%	0.60	0.265 (0.285)	1.36 (1.36)

Note: values in parenthesis indicate observed streamflow and baseflow index (BFI)

Similarly, the model validation demonstrated a satisfactory agreement between the modeled and observed streamflow for the VC watershed (Table 12). For the 2001 – 2010 validation period, the model predicted at least 62% of streamflow (p-factor = 0.62) with a low prediction uncertainty (r-factor = 0.30). Although the model performance during the validation period seemed weaker than the calibration period, the overall robustness of the model in estimating the VC streamflow is satisfactory based on the values of R^2, NSE, bR^2, KGE greater than 0.58, and a very small value of PBIAS < 0.1% (Table 12). However, despite an overall satisfactory model performance, the model could not capture some of the peak flows (Figure 12).

Figure 12. Comparison between the modeled and observed daily streamflow for the Village Creek watershed in the calibration (2011 – 2019) period

In terms of the baseflow component, the calibrated model displayed strong performance (Figure 13). Between 2001 and 2019, the BFI of the calibrated model was 0.27, which is very similar to the observations (BFI = 0.287), and much improved from the uncalibrated model (BFI = 0.328). There was an underestimation of the BFI values during the calibration (BFI = 0.261) and validation (BFI = 0.265) periods by less than 10% (Table 12) as compared to overestimation of 12 – 17% by the uncalibrated model (Table 3). Overall, the VC watershed model can be considered a reliable model in terms of its ability to partition baseflow and stormflow.

Figure 13. Comparisons of baseflow and streamflow between the model and observation in the Village Creek watershed

Water Quality: E. coli

The performance of the model to simulate *E. coli* was measured by comparing geometric means (eq. 17) of the simulated and observed *E. coli* and then calculating the overall percent bias (eq. 9) (Table 13, Figure 14). The lack of *E. coli* observations before 2011 prevented validating the modeled *E. coli* with the observations. By changing parameter values as listed in Table 8 after the model calibration, the model performance improved significantly in estimating *E. coli* concentrations in the VC watershed. The calibrated model over-predicted *E. coli* counts by only 5.6% (Table 13), which is highly improved from the over-estimation bias of 85.0% in the uncalibrated model. Therefore, the calibrated model (hereafter baseline scenario) was deemed reliable to simulate the effects of different GI scenarios on *E. coli* concentrations in the VC watershed. Out of 108 months (2011 – 2019) simulated in the baseline scenario, the *E. coli* concentration exceeded the acceptable value of 126 CFU/100mL in a total of 60 months (Figure 20).

Table 13. Performance of the calibrated Village Creek watershed model calibration in estimating E. coli

Time Period	Percent Bias	Geomean Modeled *E. coli*	Geomean Observed *E. coli*
2011-2019	5.6%	346.1	327.8

Figure 14. Modeled E. coli compared to the observed measurements collected from TCEQ.

The baseline results were analyzed to identify land cover types at the HRU level that contributed the highest to the lowest concentrations of *E. coli* to the Village Creek (Figure 15). Urban land was the highest contributor of *E. coli*, followed by rangeland, forest, and hay/pasture in the VC watershed. Of the total of 835 HRUs in the VC watershed, 472 HRUs represent urban lands. Of these, 470 urban HRUs were the major sources of *E. coli* in the watershed. Therefore, GI scenarios focused on urban areas of different degrees of imperviousness to assess the efficiency of GIs in reducing *E. coli* loads to the Village Creek.

Figure 15. E. coli concentrations as contributed by different land types in the Village Creek watershed

Scope and Application

GI Scenarios

The seven GI scenarios evaluated *E. coli* for 2011 – 2019. Then, comparing the GI scenario *E. coli* outputs with the baseline scenario demonstrated the percent change. The baseline scenario serves as a basis for the current *E. coli* condition in the watershed, with no GI practices. The model simulations under different GI scenarios indicated potential reductions in *E. coli* concentrations in the VC watershed (Table 16).

Table 14. E. coli Results of all scenarios with GI practice implementation in the Village Creek Watershed

Scenario (2011-2019)	**Average Monthly Geomean (CFU/100mL)**	**Maximum (CFU/100mL)**	**Minimum (CFU/100mL)**	**Percent Reduction**
0. Baseline	194.53	29,930.0	11.67	NA
70% bacteria removable efficiency				
1. U-70	143.38	9,152	11.68	63.1%
2. U-HD	180.61	21,050	11.67	21.9%
3. U-MD	182.05	23,580	11.68	17.9%
4. U-LD	188.62	29,280	11.67	5.0%
5. U-I	183.56	25,030	11.67	18.3%

90% bacteria removable efficiency				
6. U-90	117.14	3,215	11.68	81.1%
7. U-HD-90	176.25	18,510	11.67	28.0%

Statistical analysis revealed no significant relationship between streamflow and *E. coli* concentrations (Fig. 16) with the p-values ($t = 1.22$, $p = 0.221$). However, based on the percent bias (PBIAS = 5.6%), the model seemed acceptable to estimate *E. coli* concentrations.

Figure 16. Comparison of average monthly flow and E. coli concentrations

Scenario 1 is a hypothetical implementation of GI practices with 70% bacteria removal efficiency in urban areas in the VC watershed (32.8% of the watershed), i.e., the installation of GIs in 472 HRUs or locations in the VC watershed. Similarly, scenarios 2 to 5 represent the installation of GI practices with a 70% bacteria removal efficiency in urban areas classified as high density (7.4 % of the watershed), medium density (12.5% of the watershed), low density (12.2% of the watershed) and industrial (2.1% of the watershed). Similarly, scenarios 6 and 7 represent the installation of 90% bacteria removable efficiency on all urban and high-density urban areas in the watershed (Table 14). Scenario 1 resulted in a 63.1% reduction in *E. coli* loads followed by scenarios 2, 5, 3, and 4 with the respective *E. coli* reductions of 21.9%, 18.3%, 17.9%, and 5%. The overall *E. coli* reductions increased to 81.1% and 28% when the GI bacteria removal efficiency increased to 90%, as

represented by scenarios 6 and 7 (Table 16). Figure 17 presents the overall *E. coli* removal potential of scenario one and scenario six.

Figure 17. Reductions in E. coli concentrations under 70% and 90% reduction efficiency scenarios compared to the baseline scenario in the Village Creek watershed.

None of the scenarios tested in this study could reduce *E. coli* concentrations below the acceptable 126 CFU/100mL in all months during the simulation period. However, on average, scenario 6 (GI with 90% efficiency) reduced *E. coli* concentrations below the acceptable level in seven months (April through October). On the other hand, the GI practices with 70% efficiency (scenario 1) could only reduce concentrations in four months (June through September).

Figure 18. Reductions in the monthly geomean for E. coli concentrations from scenario 1 (70% reduction efficiency) and scenario 6 (90% reduction efficiency)

There are reductions in the peaks in *E. coli* concentrations, suggesting that implementing GI practices in these areas would greatly reduce *E. coli* counts in the VC watershed. Following the same trend as the baseline scenarios, where the streamflow and *E. coli* concentrations tend to increase around the same time (Figure 17).

The next scenarios, 2-5, identified urban land cover intensities where GI implementation may result in higher reductions than other urban areas. Scenario 2 and 7, the high-density urban areas in the watershed, reduced the amount of *E. coli* in the watershed by 21.9% and 28.0%, respectively. Scenarios 3 – 5 reduced 17.9%, 5% and 18.3% *E. coli.* These results demonstrate that the implementation of GIs in high-density urban areas is the most effective of all.

Section V. Discussion

Because the VC watershed is impaired due to elevated levels of *E. coli*, the research objective of this thesis was to develop the hydrological model of the VC watershed and then estimate the benefits of implementing GI practices in lowering *E. coli* concentrations. This study included developing the SWAT-based hydrological model of the VC watershed, using input data that included DEM, soil, slope, climate, and bacteria sources such as animal manure and septic systems. The model performed well in terms of simulating streamflow with higher correlation and lower percent bias. Although there existed no significant relationship

between streamflow and E. coli concentrations, the model's performance in simulating *E. coli* within 10% percent bias was considered satisfactory in representing VC watershed's *E. coli* condition and exploring the benefits of GI scenario implementation.

The calibrated model (baseline) showed that there existed no significant relationship between *E. coli* and streamflow. This result is in agreement with the similar results reported by Hoff and Kipatrick (2017b). It indicated that the *E. coli* discharge might not only be a result of high streamflow. It could be a result of other factors in the watershed, for example, precipitation intensity and duration, solar radiation, surface air temperature, stream water temperature, availability of nutrients, and continuous release of pollutants into the watershed instead of being discharged only during high runoff events (Petersen and Hubbart, 2020). Since there is a lack of correlation between streamflow and *E. coli*, placement of the GI practices in major source areas would be necessary for reducing concentrations, a topic of future research.

A primary concern in urban areas is high streamflow volumes discharged in the watershed, leading to high flooding in the surrounding regions. This project focuses on *E. coli* reductions in VC, and the GI practices implemented in SWAT do not address streamflow. Streamflow was crucial for model development and bacteria transport, but the GI practices directly target water quality and, in this study, *E. coli*. Based on the design, placement, and development of GI practices, there is potential for reductions in stormflow, further reducing total streamflow and chances of flooding. However, this is out of the scope of this research study. Simulations of seven GI scenarios provided estimations for GI practices' benefits in reducing *E. coli* concentrations in the watershed. The GI practices were implemented in various urban conditions at 70% bacteria reduction efficiency. Scenario 1 was all urban environments, scenario 2 was high density, scenario 3 was medium density, scenario 4 was low density, and scenario 5 was industrial areas. Additional scenarios included GI practices with a 90% efficiency, where scenario 6 was for all urban areas, and scenario 7 represented the high urban densities. The scenarios demonstrated the reductions of *E. coli* and provided insights into the needed efficiencies and places in the watershed that would prioritize implementing GI practices.

As expected, the baseline scenarios showed *E. coli* concentrations well over the TCEQ water quality requirements of 126 CFU/100mL, with an average geomean of 194.53 CFU/100mL. The urban areas impose the most stress on water quality in VC, and stakeholders should prioritize these areas for management practices that will help reduce the amount of *E. coli* transported into the VC river networks. The seven GI scenarios

demonstrated how implementing GI practices in the urban areas can target and reduce *E. coli* discharged from the watershed.

To reduce the *E. coli* concentrations to meet the TCEQ standards, GI practices with 90% bacteria removal efficiencies (scenario 6) seemed to provide relief. Implementing this aggressive scenario could reduce average monthly *E. coli* concentrations by 81.1%, bringing the average monthly geomean down to 117.14 CFU/100mL. However, this scenario still included maximum concentrations reaching 3,215 CFU/100mL, meaning there would still be instances of high *E. coli* counts. In addition, if the GI practices only effectively remove 70% of the bacteria generated in urban areas, then the watershed may still be impaired. Therefore, planners in VC should investigate GI practices that have been shown to effectively meet these reduction efficiencies, such as alum treatments, infiltration trenches, downspout drywells, and soakage trenches (Table 10) that are reported to have reduced bacteria concentrations by up to 90% (NCTCOG, 2021). Alum treatments are kinds of chemical treatment of stormwater, where infiltration trenches, downspout drywells, and soakage trenches utilize infiltration as a filter. It is important to note that these GI practices are not a one size fits all design.

An alum treatment system is a chemical treatment of stormwater, using a piped drainage system to discharge the stormwater into a wet pond mixed with liquid alum (Figure 20). The liquid alum treats the stormwater, where the reported reductions for fecal coliform and suspended solids are up to 90%, phosphorous by 80%, heavy metals by 75%, and nitrogen by 60% (NCTCOG, 2021). Awopetu et al. (2011) compared alum treatment systems to other stormwater management practices in a polluted lake. They found a 78% reduction of total fecal coliform; however, *E. coli* reduced explicitly by only 27% (Awopetu et al., 2011). According to NCTCOG, alum treatments have been shown to consistently reduce more than 99% of the fecal coliforms in stormwater (NCTCOG, 2021).

Figure 19. Alum treatment for stormwater; Site Development Controls Manual, 6.4 Alum Treatment System: Inspection and Maintenance Requirements, page. 82 (NCTCOG, 2021)

An infiltration trench, primarily designed for water quality, is a stone-filled trench that provides a space for stormwater to collect into an underground tank (Figure 21). The stormwater reaches the soil within approximately two days of a precipitation event as it filters through the trench, eventually reaching the water table. An infiltration trench filters water quality by utilizing soil and sediment's natural filtration mechanisms, with the potential for reducing fecal coliform and heavy metals up to 90%, suspended solids by 80%, and phosphorous and nitrogen by 60%. Studies have shown the benefits of infiltration-based GI practices, where they remove higher concentrations of E. coli from stormwater than chemical treatments (Jefferson et al., 2017; Wolfand et al., 2018). Not only does this aid in water quality, but these designs also recharge groundwater and maintain baseflow. These developments are suitable for residential subdivisions and high-density urban areas (NCTCOG, 2021), making this GI practice an option for placement in VC's urban and industrial areas.

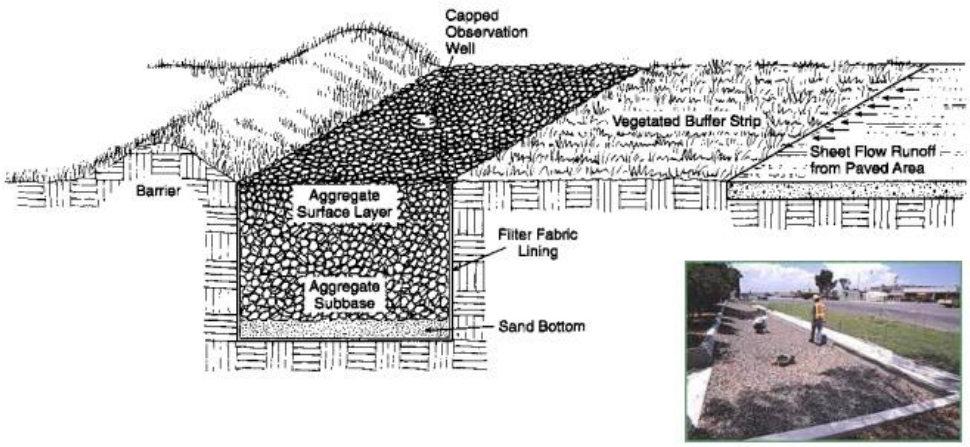

Figure 20. Infiltration trench design; Site Development Controls Manual, 20.1 Infiltration Trench General Description, page. 150 (NCTCOG, 2021)

A downspout drywell is perforated manholes that have a similar function to the infiltration trenches. However, they are a development to help reduce and treat stormflow by using minimal space, making it suitable for dense urban areas. Their water quality enhancement mechanism is similar to that of the infiltration trench. This practice reduces fecal coliform and heavy metals by 90%, suspended solids by 80%, and phosphorous and nitrogen by 60%.

Figure 21. Downspout Drywell; Site Development Controls Manual, 19.0 Downspout Drywell, page. 145 (NCTCOG, 2021)

Another GI practice reported in the SWAT manual with a bacteria efficiency of 90% is a soakage trench, which again is similar to an infiltration trench. Stormwater collected in a soakage trench is drained through the perforated pipe located within the gravel of the trench and discharged to a vegetated area. These perform the same way as the infiltration trench and downspout drywell and have the same pollutant removal efficiencies. Soakage trenches are effective in highly impervious areas, where there is limited access to soil

surface due to development.

Figure 22. Soakage Trench; Site Development Controls Manual, 21.0 Soakage Trench, page. 162 (NCTCOG, 2021)

Urban land covers are the highest contributor to E. coli in Village Creek, similar to other studies that have found urban land covers being a primary source for E. coli (Hathaway et al., 2009; Puri et al., 2009). Therefore, the urban areas should be a priority in the watershed for controlling *E. coli* sources. A critical factor discussed in the literature in identifying priority locations so the GI practices can be strategically placed in optimal performance locations throughout the study area (Di Matteo et al., 2017; Liu et al., 2017; Saadat Foomani and Malekmohammadi, 2019). Identifying these locations requires assessing topography, groundwater depth, land use types, impervious space, and locality to neighboring water bodies (Eaton, 2018; Saadat Foomani and Malekmohammadi, 2019).

Although many factors contribute to finding an optimal location, such as soil and slope, this study focused on urban areas with differing intensities when implementing GI practices to reduce amounts of *E. coli*. Prioritizing high-density urban and industrial land cover types for GI placement seemed to provide higher reductions than the other urban land cover types. It is in agreement with some studies that have shown a positive correlation between land imperviousness and E. coli concentrations and other pollutants due to the presence of higher pollutant sources in highly urbanized areas (Chen and Chang, 2014). Although only implementing GI practices in these areas would not reduce the bacteria to levels below the TCEQ standard of 126 CFU/100 mL, these areas have the highest *E. coli* reductions; therefore, they would be the most effective for achieving these standards.

Since achieving a 90% reduction is uncertain and impractical, it is essential to look at alternatives to reduce *E. coli* concentrations in the watershed. In addition, this study only targeted urban areas (about one-third

of the watershed) to test GIs' benefits; therefore, implementing GI practices in other areas, such as rangeland or grassland, could potentially enhance the bacteria reduction to the acceptable level.

Implementing GI practices in only urban areas does not achieve compliance for all E. coli measurements. VC has mixed land uses, where the major types are urban, and rangelands and urban areas were not the only E. coli sources in the watershed. Sources of E. coli were additionally in rangelands due to agricultural animals grazing. Studies have shown that management operations used to address E. coli contamination sourced from animal grazing can help reduce the amount of E. coli discharged by runoff (Voeller et al., 2021; Wilcock et al., 2009). These management operations may include manure collection, controlling stormwater, and limiting cattle's access to water bodies. Voeller et al. (2021) found that by implementing management operations that target these pollution sources in agriculture areas, average fecal indicator concentrations were reduced by 54 to 99%.

Furthermore, there was an increase in water quality measurements that met the standards (Voeller et al., 2021). Therefore, in addition to GI practices implemented in the urban areas, management operations may help control and reduce other *E. coli* in the watershed. For example, a primary source of *E. coli* in the watershed is from failing septic systems. Therefore, in addition to GI practices, another way to improve VA's water quality is by inspecting existing septic systems for potential failures and leakages and then fixing those issues. This approach could reduce the sourcing of *E. coli*. However, inspecting and repairing failing septic systems can be very expensive.

Pathogenic pollution is the leading cause of water quality impairments, polluting about 17% of the miles from assessed rivers and streams (EPA, 2017a). Of the types of pathogen fecal coliforms, *Escherichia coli (E.coli*) is the primary pollutant, causing impairments to 10% of the assessed rivers and streams in the U.S. (EPA, 2017a). Furthermore, Texas, as a state, also has water quality impairment problems. About 42% of assessed rivers and streams are classified as impaired (EPA, 2017a). The major cause of impairments is pathogenic bacteria, making up 27.5% of assessed rivers and streams (EPA, 2017a). The septic systems are a major contributor to *E. coli* loads. These are located in residential or urban areas. Failing septic systems across the U.S. release large amounts of bacteria and pollutants into surface and groundwaters (Hoff et al., 2018; Sowah et al., 2017). As this is a significant source of pollution in the urban areas, GI practices should be implemented in the regions that will capture *E. coli* before reaching the waterbodies.

Poor water quality is a threat to public health, especially pathogenic pollution, such as *E. coli*. Pathogens, including fecal coliforms, are the leading cause of water quality failing to meet standards in the U.S. (Keiser and Shapiro, 2019). Found in the intestines of warm-blooded animals, if the bacteria makes its way to surface waters, it can expose humans to these pathogens in high concentrations. There are many strains of *E. coli*, some of which are not harmful. Still, other types may result in illness and diseases such as gastrointestinal illness, respiratory pneumonia, urinary tract infections, meningitis, and gastrointestinal infections (USGS) when humans are exposed (USGS). The risk of getting sick when a person comes in contact with *E. coli* can depend on the degree of exposure (Russo et al., 2020); therefore, it is crucial to keep the concentrations low.

VC is at the headwaters of Lake Arlington, which is a freshwater supply for surrounding communities and frequently used for recreation, most popularly fishing (Hoff, 2019). Around the U.S., many people use surface waters for recreational purposes, such as swimming, sports, boating, and fishing; however, studies show that people that participate in these water recreations are put at higher risks of gastrointestinal illnesses (Deflorio-Barker et al., 2018; Russo et al., 2020). Deflorio-Barket et al. (2018) estimated that about 90 million cases of diseases (GI, respiratory, ear, eye, or skin) are from recreational use of surface waters in the U.S., polluted from pathogens such as *E. coli*. Furthermore, they estimated the annual health care cost generated from these waterborne illnesses to be about $2.9 to 3.4 billion (Deflorio-Barker et al., 2018).

Therefore, watershed managers and stakeholders must be proactive with water quality improvements. The Trinity River Authority (TRA), which monitors VC, began to take action once the impairments were noticed in 2010 before developing the Village Creek-Lake Arlington watershed protection plan. Elevated bacteria concentrations in a watershed can impose minor or severe health risks, financial burdens, and limited water use for recreation. Therefore, stakeholders must develop plans and actions to ensure the water quality is under control in the VC watershed.

Assumptions/Limitations/Future Research

There are limitations to this study regarding data, model development, and the application of management scenarios. The most important limitation is the limited availability of *E. coli* observations in the watershed. There were only 48 *E. coli* measurements available for nine years between 2011 and 2019. More importantly, the available *E. coli* measurements were sporadic, constraining our ability to train the model. Having bacteria data collected at defined regular intervals and different rainfall conditions may provide a good

training environment for model parametrization and identify relationships among other affecting variables. Therefore, future research should focus on collecting *E. coli* samples periodically through routine monitoring. For bacteria modeling analysis, bacteria sources in the watershed must be correctly identified. For example, having watershed specific cattle stocking rates, manure productions from cattle, domestic animals such as dogs, cats, and wildlife, including birds, hogs, and deer, would help estimate the appropriate amount and concentration of bacteria. This study used a county-level average stocking rate. It recommended manure productions for various wild animals as obtained from existing literature, which could not represent the VC watershed. Another important source of bacteria is the failure of wastewater infrastructure, OSSFs and sewer systems. According to the U.S. EPA, the septic system failure rate is up to 25%, with some states reaching even higher rates (EPA, 2005). Failure rate estimations for states have been as high as 50-70% in Minnesota and as low as 0.4% in Wyoming (U.S. EPA, 2002). Generally, counties in the U.S. report about 11% or 12% failure rate (Hoff et al., 2018; Withers et al., 2014). Systems over 25 to 30 years old have a higher risk of failure due to system age and lack of maintenance of these systems; however, these are more difficult to find due to the lack of permitting (EPA, 2005; Hoff et al., 2018). This study applied an OSSFs failure rate of 12%, which may not represent this watershed. For a better estimation of *E. coli* from OSSFs, future studies should identify the locations of failed systems and their failure rates for this watershed.

Land cover types and uses, including agricultural and urban areas, contribute to high E. coli concentrations in downstream waters (Gotkowska-Płachta et al., 2016; Petersen and Hubbart, 2020). In this study, a stationary land cover map was used for the entire model simulation period, which could significantly limit the dynamics of *E. coli* as their growth, concentrations, and transport are affected by varying levels of imperviousness in urban areas. Therefore, recommendations for future research include the consideration of land-use change scenarios.

This modeling research applied hypothetical management strategies to reduce bacteria concentrations. The model may overestimate E. coli removal efficiencies during high-intensity storm events, as studies have shown GI practices may lose their efficiency during more intense storms (Zhang et al., 2019). Therefore, overestimations may be greater than the typical removal of urban GI practices designed for 25-year storms. Additionally, many factors, such as design, size, placement locations, etc., go into the practical application of the GI practices, which was beyond the scope of this study. GI design is not a functionality of SWAT; however, other hydrologic models do include a design component to study the fate and transport of bacteria. For example,

the Storm Water Management Model (SWMM) can provide a much better model simulation of the GI practices' water quantity and quality performance by manipulating their structural designs (Taji and Regulwar, 2019). Future studies may utilize such models to design and place GI practices in target areas in the watershed.

The socioeconomic factors in the VC watershed may also play a role in the applicability of GI practices. This study did not evaluate stakeholders' willingness to implement and maintain different types of GI practices which can be a deciding factor for many developers (Bell et al., 2020; Herzog et al., 2019; Jayasooriya and Ng, 2013; Lee et al., 2012; Liu et al., 2016; Mao et al., 2017; Raei et al., 2019; Sohn et al., 2020). Maintenance of GI practices may be required for general functions, clogging from trash or sediments; therefore, incorporating maintenance costs is important (Herzog et al., 2019; Ishimatsu et al., 2017; Lee et al., 2015; Mao et al., 2017). NCTCOG iSWM Online Technical Manual includes cost, maintenance, and further details for the GI practices (NCTCOG, 2021). The scenarios used in this study were assumed to reduce bacteria concentrations by up to 90%, but this study did not include the cost-benefit analysis of these scenarios. However, the results of this study may provide stakeholders with insights into the potential benefits of implementing GI practices in the VC watershed.

Section VI. Conclusion

As of 2021, the VC watershed is at an impaired state due to high *E. coli* concentrations in some creek segments. This study estimated the effectiveness of GI practices to aid in *E. coli* reductions in the watershed by developing a SWAT-based hydrological model. Management scenarios with 70% and 90% *E. coli* removal efficiencies were tested under different classes of urban areas within the watershed.

Model simulations under these GI scenarios indicated their ability to reduce *E. coli* concentrations in the VC watershed by 5 to 81%. And yet, even the most aggressive scenario (Scenario 6) could only lower the *E. coli* levels below the acceptable levels of 126 CFU/100mL for 67% of the time in a nine-year model simulation period. Thus, VC watershed stakeholders may benefit by prioritizing the watershed's highly urbanized and industrial areas when planning and implementing GI practices.

Stakeholders may benefit from this research results when identifying strategies to target and reduce bacteria concentrations in the watershed. In addition, the watershed must implement strategic management practices in urban areas to restore VC's water quality to healthy standards. VC is at the headwaters of Lake Arlington, which is a primary freshwater source for surrounding communities, used for recreation, drinking

water, and other utility. As the north-central region of Texas continues to urbanize with added population, the Village Creek watershed will likely urbanize as well with added challenges of water quality. Therefore, it is crucial to maintain a healthy watershed to sustain the water resources in the area.

REFERENCES

Abbaspour, K.C. 2015 SWAT-CUP: SWAT Calibration and Uncertainty Programs (Premium Version) - A User Manual., Eawag Swiss Federal Institute of Aquatic Science and Technology.

Abbaspour, K.C., Rouholahnejad, E., Vaghefi, S., Srinivasan, R., Yang, H. and Kløve, B. 2015. A continental-scale hydrology and water quality model for Europe: Calibration and uncertainty of a high-resolution large-scale SWAT model. Journal of Hydrology 524, 733-752.

Ahmed, W., Neller, R. and Katouli, M. 2005. Evidence of septic system failure determined by a bacterial biochemical fingerprinting method. Journal of Applied Microbiology 98(4), 910-920.

Akhter, M.S. and Hewa, G.A. 2016. The Use of PCSWMM for Assessing the Impacts of Land Use Changes on Hydrological Responses and Performance of WSUD in Managing the Impacts at Myponga Catchment, South Australia. Water 8(11).

Arnold, C.L.J. and Gibbons, C.J. 1996. Impervious surface coverage: The emergence of a key environmental indicator. Journal of the American Planning Association 62(2), 243-258.

Awopetu, B., Moses, I. and Odeyemi, O. 2011. EFFICACY OF SAND FILTRATION, MORINGA OLEIFERA SEED AND ALUM TREATMENT IN REDUCTION OF COLIFORMS AND TOTAL BACTERIA IN STABILIZATION POND EFFLUENT.

Bai, Y., Zhao, N., Zhang, R. and Zeng, X. 2018. Storm Water Management of Low Impact Development in Urban Areas Based on SWMM. Water 11(1), 33.

Barker, J.C. and Walls, F.R. 2002 2002 North Carolina Agricultural Chemicals Manual: Livestock Manure Production Rates and Nutrient Content.

Bell, C.D., Wolfand, J.M., Panos, C.L., Bhaskar, A.S., Gilliom, R.L., Hogue, T.S., Hopkins, K.G. and Jefferson, A.J. 2020. Stormwater control impacts on runoff volume and peak flow: A meta-analysis of watershed modelling studies. Hydrological Processes 34(14), 3134-3152.

Brears, R.C. 2017 Urban Water Security, John Wiley & Sons, Ltd., New York.

Caldwell, P.V., Sun, G., McNulty, S.G., Cohen, E.C. and Myers, J.A.M. 2012. Impacts of impervious cover, water withdrawals, and climate change on river flows in the conterminous US. Hydrology and Earth System Sciences 16, 2839–2857.

Chen, H. and Chang, H. 2014. Response of discharge, TSS, and E. coli to rainfall events in urban, suburban, and rural watersheds. Environmental science. Processes & impacts 16 10, 2313-2324.

Coffey, R., Cummins, E., Cormican, M., Flaherty, V.O. and Kelly, S. 2007. Microbial Exposure Assessment of Waterborne Pathogens. Human and Ecological Risk Assessment: An International Journal 13(6), 1313-1351.

Debusk, K.M. and Wynn, T.M. 2011. Storm-Water Bioretention for Runoff Quality and Quantity Mitigation. Journal of Environmental Engineering 137(9), 800-808.

Deflorio-Barker, S., Wing, C., Jones, R.M. and Dorevitch, S. 2018. Estimate of incidence and cost of recreational waterborne illness on United States surface waters. Environmental Health 17(1).

Di Matteo, M., Dandy, G.C. and Maier, H.R. 2017. Multiobjective Optimization of Distributed Stormwater Harvesting Systems. Journal of Water Resources Planning and Management 143(6), 13.

Dieter, C.A., Maupin, M.A., Caldwell, R.R., Harris, M.A., Ivahnenko, T.I., Lovelace, J.K., Barber, N.L. and Linsey, K.S. 2018 Estimated use of water in the United States in 2015, p. 76, Reston, VA.

Eaton, T.T. 2018. Approach and case-study of green infrastructure screening analysis for urban stormwater control. Journal of Environmental Management 209, 495-504.

EPA, U.S. 2005 National Management Measure to Control Nonpoint Source Pollution from Urban Area: Management Measure 6: New and Existing On-Site Wastewater Treamtment System. Agency, E.P. (ed), Environmental Protection Agency, (EPA).

EPA, U.S. 2017a National Summary of State Information, U.S. Environmental Protection Agency.

EPA, U.S. 2017b Stormwater Management Practices at EPA Facilities, United States Environmental Protection Agency (EPA).

EPA, U.S. 2019 What is Green Infrastructure?, United States Environmental Protection Agency (USEPA).

Fiori, A. and Volpi, E. 2020. On the Effectiveness of LID Infrastructures for the Attenuation of Urban Flooding at the Catchment Scale. Water Resources Research 56(5), e2020WR027121.

Fry, T.J. and Maxwell, R.M. 2017. Evaluation of distributed BMPs in an urban watershedHigh resolution modeling for stormwater management. Hydrological Processes 31(15), 2700-2712.

Gotkowska-Płachta, A., Gołaś, I., Korzeniewska, E., Koc, J., Rochwerger, A. and Solarski, K. 2016. Evaluation of the distribution of fecal indicator bacteria in a river system depending on different types of land use in the southern watershed of the Baltic Sea. Environ Sci Pollut Res Int 23(5), 4073-4085.

Hagemann, S., Chen, C., Clark, D.B., Folwell, S., Gosling, S.N., Haddeland, I., Hanasaki, N., Heinke, J., Ludwig, F., Voss, F. and Wiltshire, A.J. 2013. Climate change impact on available water resources obtained using multiple global climate and hydrology models.

Haifeng Jia, Hairong Yao, Ying Tang, Shaw L. Yu, Richard Field and Tafuri, A.N. 2015. LID-BMPs planning for urban runoff control and the case study in China. Journal of Environmental Management 149, 65-76.

Hathaway, J., Hunt, W. and Jadlocki, S. 2009. Indicator Bacteria Removal in Storm-Water Best Management Practices in Charlotte, North Carolina. Journal of Environmental Engineering 135, 1275-1285.

Herzog, S.P., Eisenstein, W.A., Halpin, B.N., Portmann, A.C., Fitzgerald, N.J.M., Ward, A.S., Higgins, C.P. and McCray, J.E. 2019. Co-Design of Engineered Hyporheic Zones to Improve In-Stream Stormwater Treatment and Facilitate Regulatory Approval. Water 11(12), 18.

Hibbs, B.J. and Sharp, J.M. 2012. Hydrogeological Impacts of Urbanization. 18(1), 3-24.

Hobbie, S.E., Finlay, J.C., Janke, B.D., Nidzgorski, D.A., Millet, D.B. and Baker, L.A. 2017. Contrasting nitrogen and phosphorus budgets in urban watersheds and implications for managing urban water pollution. Proceedings of the National Academy of Sciences 114(16), 4177.

Hoff, A. 2019 Village Creek-Lake Arlington Watershed Protection Plan, p. 120, Texas Commission of Environmental Quality (TCEQ), Trinity River Authority of Texas (TRA).

Hoff, A. and Kipatrick, A. 2017a Analysis of Historical Data for the Village Creek-Lake Arlington Watershed Protection Plan, Texas Commission of Environmental Quality (TCEQ), Trinity River Authority of Texas (TRA).

Hoff, A. and Kipatrick, A. 2017b Data Collection Report for the Village Creek-Lake Arlington Watershed Protection Plan, Texas Commission of Environmental Quality (TCEQ), Trinity River Authority of Texas (TRA).

Hoff, A., Kipatrick, A., Mangham, W. and Hauck, L. 2018 Technical Report on Source Identification and Load Reduction Evaluation for the Village Creek-Lake Arlington Watershed Protection Plan, Texas Commission of Environmental Quality (TCEQ), Trinity River Authority of Texas (TRA).

Houng Li, Lucas J. Sharkey, William F. Hunt and Allen P. Davis 2009. Mitigation of Impervious Surface Hydrology Using Bioretention in North Carolina and Maryland. Journal of Hydrologic Engineering 14(4).

Hu, S. and Shrestha, P. 2020. Examine the impact of land use and land cover changes on peak discharges of a watershed in the midwestern United States using the HEC-HMS model. Papers in Applied Geography 6(2), 101-118.

Iqbal, M.S. and Hofstra, N. 2019. Modeling Escherichia coli fate and transport in the Kabul River Basin using SWAT. Human and Ecological Risk Assessment: An International Journal 25(5), 1279-1297.

Ishimatsu, K., Ito, K., Mitani, Y., Tanaka, Y., Sugahara, T. and Naka, Y. 2017. Use of rain gardens for stormwater management in urban design and planning. Landsc. Ecol. Eng. 13(1), 205-212.

Jaber, F. 2015 Dallas Urban Center Stormwater BMPs. Research, T.A.M.A. (ed), Texas Commission on Environmental Quality.

Jayasooriya, V.M. and Ng, A.W.M. (2013) Development of a framework for the valuation of Eco-System Services of Green Infrastructure, Modelling & Simulation Soc Australia & New Zealand Inc, Christchurch.

Jefferson, A.J., Bhaskar, A.S., Hopkins, K.G., Fanelli, R., Avellaneda, P.M. and McMillan, S.K. 2017. Stormwater management network effectiveness and implications for urban watershed function: A critical review. Hydrological Processes 31(23), 4056-4080.

Jeong, J., Wagner, K., Flores, J.J., Cawthon, T., Her, Y., Osorio, J. and Yen, H. 2019. Linking watershed modeling and bacterial source tracking to better assess E. coli sources. Science of The Total Environment 648, 164-175.

Knisel, W.G. 1980. A Field Scale Model for Chemical, Runoff, and Erosion from Agricultural Management Systems. . Conservation Service Report 26.

Knoben, W.J.M., Freer, J.E. and Woods, R.A. 2019. Technical note: Inherent benchmark or not? Comparing Nash–Sutcliffe and Kling–Gupta efficiency scores. Hydrology and Earth System Sciences 23(10), 4323-4331.

Konrad, C.P. 2016 Effects of Urban Development on Floods.

Kurtz, T. 2009 Flow monitoring of three ecoroofs in Portland, Oregon.

Lee, J.G., Borst, M., Brown, R.A., Rossman, L. and Simon, M.A. 2015. Modeling the Hydrologic Processes of a Permeable Pavement System. Journal of Hydrologic Engineering 20(5), 12.
Lee, J.G., Selvakumar, A., Alvi, K., Riverson, J., Zhen, J.X., Shoemaker, L. and Lai, F.H. 2012. A watershed-scale design optimization model for stormwater best management practices. Environ. Modell. Softw. 37, 6-18.
Levin, R.B., Epstein, P.R., Ford, T.E., Harrington, W., Olson, E. and Reichard, E.G. 2002. U.S. drinking water challenges in the twenty-first century. Environmental Health Perspectives 110(suppl 1), 43-52.
Lian, Q., Yao, L., Uddin Ahmad, Z., Lei, X., Islam, F., Zappi, M.E. and Gang, D.D. 2019. Nonpoint source pollution. Water Environment Research 91(10), 1114-1128.
Lim, K.J., Engel, B.A., Tang, Z., Choi, J., Kim, K.-S., Muthukrishnan, S. and Tripathy, D. 2005. AUTOMATED WEB GIS BASED HYDROGRAPH ANALYSIS TOOL, WHAT. Journal of the American Water Resources Association 41(6), 1407-1416.
Liu, Y., Bralts, V.F. and Engel, B.A. 2015. Evaluating the effectiveness of management practices on hydrology and water quality at watershed scale with a rainfall-runoff model. Science of The Total Environment 511, 298-308.
Liu, Y.Z., Engel, B.A., Collingsworth, P.D. and Pijanowski, B.C. 2017. Optimal implementation of green infrastructure practices to minimize influences of land use change and climate change on hydrology and water quality: Case study in Spy Run Creek watershed, Indiana. Science of the Total Environment 601, 1400-1411.
Liu, Y.Z., Theller, L.O., Pijanowski, B.C. and Engel, B.A. 2016. Optimal selection and placement of green infrastructure to reduce impacts of land use change and climate change on hydrology and water quality: An application to the Trail Creek Watershed, Indiana. Science of the Total Environment 553, 149-163.
Mao, X.H., Jia, H.F. and Yu, S.L. 2017. Assessing the ecological benefits of aggregate LID-BMPs through modelling. Ecol. Model. 353, 139-149.
Martin-Mikle, C.J., De Beurs, K.M., Julian, J.P. and Mayer, P.M. 2015. Identifying priority sites for low impact development (LID) in a mixed-use watershed. Landscape and Urban Planning 140, 29-41.
Monteith, J.L. 1965. Evaporation and Environment. Symposia of the Society for Experimental Biology 19, 205-234.
NCTCOG 2016 North Central Texas Floods May-June 2015, North Central Texas Council of Governments (NCTCOG).
NCTCOG 2021 iSWM Online Technical Manual: Site Development Controls, North Central Texas Council of Governments.
Neitsch, S.L., Arnold, J.G., Kiniry, J.R. and Williams, J.R. 2011 Soil and Water Assessment Tool: Theoretical Documentation: Version 2009, Texas Water Resources Institute
Nguyen, H., Recknagel, F. and Meyer, W. 2018. Water Quality Control Options in Response to Catchment Urbanization: A Scenario Analysis by SWAT. Water 10(12), 1846.
Nguyen, T.T., Ngo, H.H., Guo, W.S., Wang, X.C.C., Ren, N.Q., Li, G.B., Ding, J. and Liang, H. 2019. Implementation of a specific urban water management - Sponge City. Science of the Total Environment 652, 147-162.
Osman, M., Wan Yusof, K., Takaijudin, H., Goh, H.W., Abdul Malek, M., Azizan, N.A., Ab. Ghani, A. and Sa'Id Abdurrasheed, A. 2019. A Review of Nitrogen Removal for Urban Stormwater Runoff in Bioretention System. Sustainability 11(19), 5415.
Parajuli, P.B. (2007) SWAT Bacteria Sub-Model Evaluation and Application Kansas State University
Petersen, F. and Hubbart, J.A. 2020. Quantifying Escherichia coli and Suspended Particulate Matter Concentrations in a Mixed-Land Use Appalachian Watershed. Water 12(2), 532.
Pierson, S.T., Cabrera, M.L., Evanylo, G.K., Schroeder, P.D., Radcliffe, D.E., Kuykendall, H.A., Benson, V.W., Williams, J.R., Hoveland, C.S. and McCann, M.A. 2001. Phosphorus Losses from Grasslands Fertilized with Broiler Litter: EPIC Simulations. Journal of Environmental Quality 30(5), 1790-1795.
Pistocchi, A. 2020. A preliminary pan-European assessment of pollution loads from urban runoff. Environmental Research 182, 109129.
Puri, D., Karthikeyan, R. and Babbar-Sebens, M. 2009. Predicting the Fate and Transport ofE. coliin Two Texas River Basins Using a Spatially Referenced Regression Model. JAWRA Journal of the American Water Resources Association 45(4), 928-944.
Raei, E., Alizadeh, M.R., Nikoo, M.R. and Adamowski, J. 2019. Multi-objective decision-making for green infrastructure planning (LID-BMPs) in urban storm water management under uncertainty. Journal of Hydrology 579, 13.

Renner, M., Brust, K., Schwarzel, K., Volk, M. and Bernhofer, C. 2014. Separating the effects of changes in land cover and climate: a hydro-meteorological analysis of the past 60 yr in Saxony, Germany. Hydrology and Earth System Sciences 18, 389-405.
Rezaei, A.R., Ismail, Z., Niksokhan, M.H., Dayarian, M.A., Ramli, A.H. and Shirazi, S.M. 2019. A Quantity–Quality Model to Assess the Effects of Source Control Stormwater Management on Hydrology and Water Quality at the Catchment Scale. Water 11(7), 1415.
Roser, M. 2020 Future Population Growth, Our World in Data.
Russo, G.S., Eftim, S.E., Goldstone, A.E., Dufour, A.P., Nappier, S.P. and Wade, T.J. 2020. Evaluating health risks associated with exposure to ambient surface waters during recreational activities: A systematic review and meta-analysis. Water Res 176, 115729.
Saadat Foomani, M. and Malekmohammadi, B. 2019. Site selection of sustainable urban drainage systems using fuzzy logic and multi-criteria decision-making. Water and Environment Journal.
Sadeghi, A. and Arnold, J. 2002. A SWAT/Microbial Sub-Model for Predicting Pathogen Loadings in Surface and Groundwater at Watershed and Basin Scales. Total Maximum Daily Load (TMDL) Environmental Regulations.
Saraswat, C., Kumar, P. and Mishra, B.K. 2016. Assessment of stormwater runoff management practices and governance under climate change and urbanization: An analysis of Bangkok, Hanoi and Tokyo. Environmental Science & Policy 64, 101-117.
Shao, M., Zhao, G., Kao, S.-C., Cuo, L., Rankin, C. and Gao, H. 2020. Quantifying the effects of urbanization on floods in a changing environment to promote water security — A case study of two adjacent basins in Texas. Journal of Hydrology 589, 125154.
Shiqiang Du, P.S., Anton Van Rompaey, Jiahong Wen 2015. Quantifying the impact of impervious surface location on flood peak discharge in urban areas. Natural Hazards 76, 1457-1471.
Sidhu, J.P.S., Ahmed, W., Gernjak, W., Aryal, R., McCarthy, D., Palmer, A., Kolotelo, P. and Toze, S. 2013. Sewage pollution in urban stormwater runoff as evident from the widespread presence of multiple microbial and chemical source tracking markers. Sci Total Environ 463-464, 488-496.
Sohn, W., Kim, H.W., Kim, J.H. and Li, M.H. 2020. The capitalized amenity of green infrastructure in single-family housing values: An application of the spatial hedonic pricing method. Urban For. Urban Green. 49, 10.
Soil Conservation Service, S. 1972 Section 4: Hydrology in National Engineering Handbook SCS.
Sowah, R.A., Habteselassie, M.Y., Radcliffe, D.E., Bauske, E. and Risse, M. 2017. Isolating the impact of septic systems on fecal pollution in streams of suburban watersheds in Georgia, United States. Water Research 108, 330-338.
Taji, S.G. and Regulwar, D.G. 2019. LID coupled design of drainage model using GIS and SWMM. ISH Journal of Hydraulic Engineering.
TCEQ 2012 Chapter 4: Collection and Analyzing Bacteriological Samples, Texas Commission on Environmental Quality.
TRA 2008 2008 Basin Highligts Report. (TRA), T.R.A. (ed), Texas Commission on Environmental Quality.
U.S. EPA 2002 Onsite Wastewater Treatment Systems Manual U.S. Environmental Protection Agency
U.S. EPA 2017 National Water Quality Inventory: Report to Congress, Environmental Protection Agency.
United Nations 2019 World Urbanization Prospects: The 2018 Revision. Department of Economic and Social Affairs, P.D. (ed), p. 126, United Nations, New York.
USDA Animal Manure Management United States Department of Agriculture.
USGS Bacteria and E. coli in Water, usgs.gov.
VNT 2010 North Texas 2050, Vision North Texas (VNT).
Voeller, D.J., Ketcham, B.J. and Becker, B.H. 2021. Improved Microbial Water Quality Associated with Best Management Practices on Coastal Dairies and Livestock Grazing Operations. Rangeland Ecology & Management 76, 139-149.
Wen Liu, W.C., Chi Peng 2014. Assessing the effectiveness of green infrastructures on urban flooding reduction: A community scale study. Ecological Modeling 291, 6-14.
Wilcock, R.J., Betteridge, K., Shearman, D., Fowles, C.R., Scarsbrook, M.R., Thorrold, B.S. and Costall, D. 2009. Riparian protection and on-farm best management practices for restoration of a lowland stream in an intensive dairy farming catchment: A case study. New Zealand Journal of Marine and Freshwater Research 43(3), 803-818.
Withers, P.J., Jordan, P., May, L., Jarvie, H.P. and Deal, N.E. 2014. Do septic tank systems pose a hidden threat to water quality? Frontiers in Ecology and the Environment 12(2), 123-130.

Wolfand, J.M., Bell, C.D., Boehm, A.B., Hogue, T.S. and Luthy, R.G. 2018. Multiple Pathways to Bacterial Load Reduction by Stormwater Best Management Practices: Trade-Offs in Performance, Volume, and Treated Area. Environmental Science & Technology 52(11), 6370-6379.
Zhang, Z.Y., Gu, J.J., Zhang, G.S., Ning, P., Ma, W.J., Zhao, L., Shen, J. and Iop (2019) 2018 4th International Conference on Environmental Science and Material Application, Iop Publishing Ltd, Bristol.

VITA

Holly Anne Gould was born June 25, 1996, in Newport News, Virginia. She is the daughter of Dr. Elaine Gould and Dr. Dana Gould. After graduating from Poquoson High School in 2014, she received a Bachelor of Science degree with a major in marine sciences, emphasizing coastal resources management and marine policy, from the University of South Carolina in 2018. After receiving her Bachelor of Science degree, she worked as a project participant, and project lead for the NASA DEVELOP Program in Hampton, Virginia.

In August 2019, she began graduate school at Texas Christian University in Fort Worth, Texas. While working on her master's degree in environmental sciences, she held a teaching assistant position for the environmental sciences department. Holly received her Master of Science degree in August 2021.

ABSTRACT

MODELING THE IMPACTS OF GREEN INFRASTRUCTURE ON *E. COLI* IN THE VILLAGE CREEK WATERSHED, TEXAS

by Holly Anne Gould, 2021
Department of Environmental Sciences
Texas Christian University

Thesis Advisor: Gehendra Kharel, Assistant Professor of Environmental Science

Urbanization imposes threats to water quality requiring water management strategies that aid sustainable development, such as green infrastructure (GI). This study estimated the usefulness of GI practices to help in *E. coli* reductions in an impaired Village Creek watershed (VC) located in the North Central Texas region. First, a Soil and Water Assessment Tool-based model of the VC was developed to represent current watershed conditions. Then, seven GI scenarios, with 70% and 90% bacteria removal efficiencies, were implemented in urban areas to estimate their impacts in reducing *E. coli* concentrations. The results showed that the GI scenario with 90% removal efficiency could reduce about 81% *E. coli* concentrations in the watershed, with higher reductions observed in high-density and industrial urban areas. Thus, the findings of this thesis research could be beneficial to stakeholders in the VC watershed to reduce *E. coli* concentrations through GI implementations in target areas.